PHYSICAL REVIEW B VOLUME 44, NUMBER 22 1 DECEMBER 1991-II

Discrete-state models of orientational glasses

H. Vollmayr, R. Kree, and A. Zippelius
Institut für Theoretische Physik, Universität Göttingen, Bunsenstrasse 9, D-3400 Göttingen, Germany

(Received 3 June 1991)

We construct and study a class of models for crystalline systems which undergo structural changes due to the cooperative freezing of orientable defects. The defects are assumed to possess uniaxial symmetry and are located on randomly chosen sites of a deformable cubic lattice. The orientations of the defects are restricted by lattice anisotropies. We consider three possibilities with discrete sets of allowed orientations. The defect axis may be parallel to (a) the cubic axes, (b) the space diagonals of the cube, or (c) the face diagonals of the cube. For quadrupolar defects the phase diagram and the elastic properties of the emerging three-state (case a), four-state (case b), and six-state (case c) model are studied, with the coupling between defects in mean-field approximation. In addition, we obtain results for a model of dipolar defects with three orientations, which is related to the six-state model. Depending on the degree of disorder, we find either states with long-range orientational order and uniform lattice distortions or glassy states. The freezing of defect orientations into a homogeneously ordered state is accompanied by enhanced fluctuations and a pronounced softening of the lattice in symmetry directions, which are determined by the lattice-anisotropy fields. We conclude that the models correctly describe essential experimental findings for orientational glasses.

I. INTRODUCTION

The present study is motivated by the large variety of experimental realizations of crystalline systems with orientable defects and substitutional disorder.[1] In most of these systems one observes a cooperative freezing into an orientational glass state, which is reminiscent of the spin-glass transition in disordered magnetic materials.[2] Since the orientational degrees of freedom are coupled to lattice distortions,[3] the random freezing gives rise to local static strains. Hence the low-temperature phase has features of a structural glass. From a theoretical point of view, such systems are of interest, because they combine elements of spin glasses, for which the model building is well understood, with properties of structural glasses, which have not yet been modeled adequately.

In this paper we suggest a class of mesoscopic models for orientational glasses. The orientational degrees of freedom are modeled as discrete state variables. The number of states and the symmetry of their interaction is determined by the local anisotropy and the crystal structure.[4] For example, cubic symmetry is compatible with an anisotropic six-state model, if the anisotropy favors the six face diagonals for the orientation of the defect. The interaction has a uniform and a random component giving rise to long-range ordered phases and glasslike phases, much like in spin-glass models of disordered magnets.[2] We focus here on the phase diagram, the symmetry of the low-temperature phase, and the critical behavior of orientational and elastic degrees of freedom. Phenomena, which are specific for very low temperatures,[5–7] shall not be considered.

As compared to magnetic systems, the orientational glasses show a much larger variety of phases. Furthermore the coupling of orientations to lattice distortions is essential to understanding the elastic properties of these systems. Long-range orientational order always gives rise to a uniform lattice distortion. In the above example this can be rhombohedral, orthorhombic, or tetragonal. The glassy phase is characterized by freezing of the orientations into random directions, giving rise to local static lattice deformations. Just like the cubic symmetry is broken globally into rhombohedral, orthorhombic, or tetragonal symmetry in the long-ranged ordered phase, it can be broken locally in various ways in the glassy phase. In the above example we predict two glassy phases, one with local tetragonal order and one with local orthorhombic order.

The paper is organized as follows. In Sec. II we discuss the model building. We consider defects with uniaxial symmetry (quadrupoles), which are modeled as three-, four-, or six-state variables—depending on the local anisotropy. In Sec. III we derive exact relations between strain and orientation correlations. These exact relations are a direct consequence of the bilinear coupling between strain fields and orientations in our model. The phase diagrams for the three- and four-state models are derived in Sec. IV. Subsequently we discuss the changes in the crystal structure and the elastic properties of the low-temperature phases (Sec. V). The quadrupolar six-state model is analyzed in Sec. VI, while in Sec. VII we show that the same model also applies to a dipolar system with three easy axes. The main results are summarized and related to experiment in Sec. VIII.

II. MODEL BUILDING

In this section we introduce a class of models for systems of immobile, orientable defects randomly located in a deformable crystal lattice. Prominent examples of such systems are disordered mixed alkali halide–alkali cyanide crystals, potassium tantalate crystals doped with Li, Na, or Nb, and argon-nitrogen mixed crystals.[1] For the mixed alkali halides–alkali cyanides much work has been spent on the model building starting from microscopic lattice dynamics.[3,8,9] Although the models discussed below are based on some principles which arose from this work, we do not aim at a description of specific substances at microscopic length scales. Our major interest is focused on phase transitions with diverging (or at least large) correlation lengths induced by ordering and freezing of the defect orientations. Other possible mechanisms for structural or martensitic transitions will not be considered here.

Our aim is to construct a semimicroscopic model for mixed crystals. For that purpose it is instructive to first consider the microscopic Hamiltonian of systems of the type $(AD)_{1-x}(AB)_x$, where D is a rigid orientable defect or molecule. We assume that the pure AB crystal has cubic symmetry and that D has uniaxial symmetry, so that its orientational configurations can be characterized by a unit vector $\mathbf{d}$. All the above-mentioned systems belong to this class. In the mixed alkali halides/cyanides, e.g., A is an alkali metal atom (Na,K,Rb,Cs) and B ($=$ Br, Cl, I) a halogen atom, whereas D are the dumbbell-shaped CN$^-$ molecular ions, which randomly replace the halogen atoms.

Microscopic model building starts from a system of atoms and defects (molecules) occupying the lattice sites of the stable high-temperature phase and interacting via two-body potentials $v_{\alpha\beta}$ ($\alpha,\beta = A$, B, or D). Quenched disorder is represented by variables n_i, which take on the value 1 if a site $\mathbf{r}_i$ is occupied by a D and $n_i = 0$ otherwise. The actual positions $\mathbf{r}_i$ are characterized by displacements $\mathbf{u}_i$ from ideal reference lattice points $\mathbf{R}_i^0$, i.e., $\mathbf{r}_i = \mathbf{R}_i^0 + \mathbf{u}_i$. There is some arbitrariness in choosing the reference lattice. Let us start from the lattice of the pure AB crystal. Then the total potential energy of the mixed crystal can be written in the form

$$H = U_{AB} + \Delta U_{DA} + \Delta U_{DB} + \Delta U_{DD}\,, \tag{1}$$

where U_{AB} corresponds to the potential energy of the pure AB crystal and the other terms are sums over two-body excess potentials $\Delta v_{D\alpha}(\mathbf{r}_i,\mathbf{r}_j,\mathbf{d}_i) \equiv v_{D\alpha}(\mathbf{r}_i,\mathbf{r}_j,\mathbf{d}_i) - v_{B\alpha}(\mathbf{r}_i,\mathbf{r}_j)$ for $\alpha =$ A or B and $\Delta v_{D,D} \equiv v_{D,D} - v_{B,B}$. A straightforward expansion of H in powers of displacements $\mathbf{u}_i$ reveals the following structure:

$$\begin{aligned} H = {} & H_{AB}^{(2)} + \tfrac{1}{2}\sum_{ij} n_i \mathbf{u}_i^T \mathbf{M}_{ij}(\mathbf{d}_i, n_j\mathbf{d}_j)\mathbf{u}_j + \sum_{ij} n_i(1-n_j)\mathbf{A}_{ij}(\mathbf{d}_i)(\mathbf{u}_i - \mathbf{u}_j) \\ & + \tfrac{1}{2}\sum_{ij} n_i n_j \big(B_{ij}(\mathbf{d}_i,\mathbf{d}_j) + \mathbf{D}_{ij}(\mathbf{d}_i,\mathbf{d}_j)(\mathbf{u}_i - \mathbf{u}_j)\big) + \sum_{j} n_i F_i(\mathbf{d}_i) + \text{anharmonic terms.} \end{aligned} \tag{2}$$

The summation extends over the lattice sites $\mathbf{R}_i^0$. All the terms appearing in (2) are easily interpreted. $H_{AB}^{(2)}$ is the harmonic approximation of U_{AB} and the next term on the right-hand side of (2) originates from the modifications of harmonic couplings in the mixed crystal. The third term arises from the forces, by which a defect causes displacements of surrounding A and B atoms from their idealized reference lattice sites. $F_i(\mathbf{d}_i)$ is the anisotropy potential that a defect experiences in a rigid lattice. Finally, $B_{ij}(\mathbf{d}_i,\mathbf{d}_j)$ denotes the direct interaction between defects in a rigid lattice and $\mathbf{D}_{ij}$ takes into account the corrections of this interaction due to lattice displacements.

In the following we do not aim at a microscopic calculation. Hence the details of the derivation of Eq. (2) are not presented. The microscopic Hamiltonian will be used in the following only as a guideline for the coarse-graining procedure. At present there is no attempt to treat a model including all these terms simultaneously. All the models considered up to now invoke some kind of phenomenological coarse-graining procedure to extract long-wavelength properties from (1) or (2). There are two reasons why such a procedure is unavoidable.

(i) The quenched randomness leads to large fluctuations of all the terms in (2) on microscopic length scales. Therefore the standard textbook procedures[10] to extract long-wavelength, elastic properties (e.g., by gradient expansions) cannot be used here. A complete theoretical treatment of a harmonic Hamiltonian with random dynamical matrix and random couplings to orientational degrees of freedom is not available.

(ii) The reorientation of a defect is a strongly anharmonic process on microscopic length scales.[11] Thus the anharmonic terms have to be taken into account. Their effects are hard to estimate from first principles in a disordered medium.

In this work we consider regions of thermodynamic parameters where the correlation length ξ of thermal orientational fluctuations is already much larger than the lattice constant, i.e., $\xi \gg a$. The coarse-graining procedure should lead to an effective Hamiltonian for the long-wavelength fluctuations which drive the phase transition under consideration. In accordance with the theory of critical phenomena, we study the simplest effective Hamiltonian which can give rise to the observed symmetry changes[12] and is compatible with (2). The form of H_{eff} is restricted by the following three simplifying assumptions.

(i) The ranges of all interatomic forces are short as compared to the mesoscopic coarse-graining length ξ_0 ($a \ll \xi_0 \ll \xi$), with the possible exception of direct interactions between defects due to electrical multipoles.

Thus H_{eff} should consist of terms which are local in the coarse-grained displacement field $\mathbf{u}(x)$ and their derivatives.

(ii) On mesoscopic length scales the system behaves as an elastic medium so that H_{eff} is at most quadratic in $\mathbf{u}(x)$. Note that this does not imply the harmonic approximation at shorter length scales.

(iii) The local anisotropy of the high-temperature lattice effectively restricts orientational fluctuations to a discrete set of states in the vicinity of a phase transition. The discrete states correspond to the absolute minima of the anisotropy potential on the length scale ξ. Note that this potential is not the microscopic anisotropy as represented by $F_i(\mathbf{d}_i)$ in (2). The positions of the absolute minima may change when approaching the transition and ξ becomes larger. Therefore the relevant discrete set of orientations cannot always be extracted from high-temperature data. As a calculation of the anisotropy requires a theoretical analysis on microscopic length scales, we can only assume a certain set of orientations and compare our results with experiments to find out whether or not the assumed anisotropy is realized in a specific substance. We should also note that the region of validity of a model with a fixed set of orientations may become limited if the anisotropy potential changes its form dramatically in the vicinity of the phase transition.

Given these three simplifying assumptions, the simplest effective Hamiltonian takes on the form

$$H_{\text{eff}} = \sum_{x} \Big\{ \tfrac{1}{2}\epsilon_{ij}(x) C^0_{ijkl}\epsilon_{kl}(x) + \sigma_{ij}(\mathbf{d}(x))\epsilon_{ij}(x) + v(\mathbf{d}(x)) \Big\} + \tfrac{1}{2}\sum_{xx'} J_{xx'}(\mathbf{d}(x),\mathbf{d}(x')). \quad (3)$$

The x summations extend over the points of a coarse-grained lattice with cubic point-group symmetry. We could have written (3) alternatively as integrals over the slowly varying fields $\epsilon_{ij}(x), \mathbf{d}(x)$ which have to be regularized by a cutoff. In (3) we have chosen a regularization in real space which automatically respects the cubic point-group symmetry. Furthermore a summation convention with respect to Cartesian indices $i,j,\ldots = \{1,2,3\}$ is implied; $\epsilon_{ij} \equiv (\partial_i u_j + \partial_j u_i)/2$ is the (coarse-grained) local strain tensor and $\sigma_{ij}(\mathbf{d}(x))$ denotes the local stress arising from a defect in the orientational state $\mathbf{d}(x)$. $\sigma_{ij}(\mathbf{d})$ is a coarse-grained version of the Kanzaki force dipole tensor.[13] The coupling term $\sim \sigma_{ij}\epsilon_{ij}$ corresponds to the terms $\mathbf{A}_{ij}(\mathbf{d}_i)$ in the harmonic approximation (2). The C^0_{ijkl} are the bare elastic constants on the mesoscopic coarse-graining scale. $v(\mathbf{d}(x))$ denotes the local anisotropy. The coupling $J_{xx'}(\mathbf{d}(x),\mathbf{d}(x'))$ between defects will in general contain contributions from direct electrical multipole interactions as well as indirect interactions via lattice distortions on the short length scales $l < \xi_0$ which have been eliminated during the coarse graining. The coupling term is nonlocal because these interactions decrease with a power-law decay for large separations and therefore cannot be considered short ranged.[14] The quenched random positions of the defects will lead to random couplings $J_{xx'}$ on the coarse-grained lattice.[8,4] The quadrupolar interactions between two defects in a homogeneous elastic medium will tend to order the defect orientations antiferromagnetically in a "tee" configuration with one axis parallel and one axis perpendicular to the vector between the defect locations. This will lead to frustration if the defects occupy sites of a three-dimensional Bravais lattice. In a medium with a finite concentration of randomly located defects on a lattice a certain fraction of defect pairs will interact ferromagnetically, favoring the parallel alignment of orientations.[5] Thus the defect coupling has the essential properties of spin-glass models, i.e., frustration and a random mixture of ferro- and antiferromagnetic bonds.[2]

Before we proceed with the discussion of Eq. (3) let us remark that many additional terms will arise as a result of coarse graining. The second term on the right-hand side of Eq. (2), e.g., will lead to couplings $c_{ijklm}\epsilon_{ij}\epsilon_{kl}f_m(\mathbf{d})$ and others. Furthermore, the functions $\sigma_{ij}(\mathbf{d})$ and $v(\mathbf{d})$ will in general also acquire quenched random fluctuations $\delta\sigma_{ij}(\mathbf{d}(x),x)$ and $\delta v_{ij}(\mathbf{d}(x),x)$, whereas in Eq. (3) the only random term is the direct coupling between defects. Some of the additional couplings have been used in other theoretical approaches to the orientational glass state[16] and the phase diagrams of mixed crystals.[17,18] In this work we consider the effective Hamiltonian equation (3) as a generic model for ordering and freezing phenomena of orientable defects in crystals, in the sense that it implies phase transitions to noncubic and glassy phases. Additional terms, which do not modify these transitions qualitatively will be considered as irrelevant, even if they lead to large quantitative modifications of the transition temperatures, critical defect concentrations, etc.

Let us continue the discussion of the model building with the specification of the anisotropy potential $v(\mathbf{d})$ in Eq. (3). In the following we want to consider potentials which possess absolute minima in the directions of an equivalent set of cubic symmetry axes, i.e., in the directions of

(A) the three fourfold axes which are parallel to the cubic axes or

(B) the four threefold axes parallel to the body diagonals of the cube or

(C) the six twofold axes parallel to the face diagonals of the cube.

These cases are realized as microscopic anisotropy potentials, if the interactions do not extend beyond nearest or next-nearest neighbors, respectively. In Refs. 3 and 8 it was shown that, e.g., cyanide-halide attractive (repulsive) nearest-neighbor interactions lead to type A (B) microscopic anisotropies. Type C can be realized, if next-nearest neighbors are also taken into account. Therefore, we consider A, B, and C as the simplest prototype anisotropies and assume that they are still present on the mesoscopic scale, i.e., in $v(\mathbf{d})$. More general cases can be studied, if this should be required by experimental data.

If the defects do not have a dipole moment (like the N_2 molecule in argon and—as a first approximation—the CN^- in the alkali halides–alkali cyanides) $\mathbf{d}$ and $-\mathbf{d}$ are equivalent and $v(\mathbf{d})$ restricts the orientational fluctuations to three (A), four (B), or six (C) states corresponding to the symmetry axes. Let us number these orientations by $\mu, \nu = 1, \ldots, p$ ($p = 3$, 4, or 6) and introduce variables $n^\mu(x)$ which are equal to 1 if the defect at x is in the orientational state μ and which are equal to zero otherwise. The effective Hamiltonian for the discrete state fluctuations takes on the form

$$H_{\text{eff}} = \sum_x \left\{ \tfrac{1}{2}\epsilon(x)\mathrm{C}^0\epsilon(x) + \sum_\mu^p n^\mu(x)\boldsymbol{\sigma}^\mu\epsilon(x) \right\} - \tfrac{1}{2}\sum_{x,x'}\sum_{\mu\nu}^p J^{\mu\nu}_{xx'} n^\mu(x) n^\nu(x'). \tag{4}$$

Cubic symmetry restricts the form of all couplings in H_{eff}. There are only three independent elastic constants: C^0_{1111}, C^0_{1122}, and C^0_{1212}. The extra stresses (force-dipole tensors) of uniaxial defects are denoted by $\boldsymbol{\sigma}^\mu$. As the defect axes coincide with cubic symmetry axes for models A, B, and C, $\boldsymbol{\sigma}^\mu$ has to be invariant against residual symmetry operations (e.g., rotations around the defect axis which leave the cube invariant). Thus, symmetry reduces the $\boldsymbol{\sigma}^\mu$ to the following form:

Model A, defect axis $\parallel \mathbf{d} = (1,0,0)$

$$\boldsymbol{\sigma}^1 = \begin{pmatrix} \sigma_0 + \frac{2}{3}\sigma & 0 & 0 \\ 0 & \sigma_0 - \frac{1}{3}\sigma & 0 \\ 0 & 0 & \sigma_0 - \frac{1}{3}\sigma \end{pmatrix}. \tag{5}$$

Model B, defect axis $\parallel \mathbf{d} = (1,-1,-1)$

$$\boldsymbol{\sigma}^1 = \begin{pmatrix} \sigma_0 & -\sigma & -\sigma \\ -\sigma & \sigma_0 & +\sigma \\ -\sigma & +\sigma & \sigma_0 \end{pmatrix}. \tag{6}$$

Model C, defect axis $\parallel \mathbf{d} = (0,1,1)$

$$\boldsymbol{\sigma}^1 = \begin{pmatrix} \sigma_0 + 2\sigma_L & 0 & 0 \\ 0 & \sigma_0 - \sigma_L & \sigma_T \\ 0 & \sigma_T & \sigma_0 - \sigma_L \end{pmatrix}. \tag{7}$$

All the other $\boldsymbol{\sigma}^\mu$ can be obtained from Eqs. (5)–(7) by applying those symmetry operations which do not leave $\boldsymbol{\sigma}^1$ invariant. Note that we have parametrized the extra stresses in a form which explicitly splits them into isotropic pressure and shear stresses, i.e., $\sigma^\mu_{ij} = \sigma_0\delta_{ij} + \tilde{\sigma}^\mu_{ij}$. Each defect will in general act as a center of dilatation and therefore a finite defect concentration leads to a change of the lattice constant. In our coarse-grained model this effect is contained in the isotropic pressure terms as can be seen by inserting $\sigma_0\delta_{ij}$ for $\boldsymbol{\sigma}^\mu$ in Eq. (4) and using $\sum_\mu n^\mu(x) = 1$. The coupling term takes on the form $\sigma_0 \sum_{x,i} \epsilon_{ii}(x)$. It can be compensated for by an appropriate shift $\epsilon_{ii} \to \epsilon_{ii} - (C^0_{1111} + 2C^0_{1122})^{-1}\sigma_0/2$ which corresponds to a readjustment of the lattice constant. To avoid extra notations we will always denote strains with respect to any reference lattice by the same symbol ϵ. Note that $\sum_i \tilde{\sigma}^\mu_{ii} = 0$ and $\sum_\mu \tilde{\boldsymbol{\sigma}}^\mu = 0$.

The ensemble of random couplings $J^{\mu\nu}_{xx'} = J^{\nu\mu}_{xx'}$ also has to respect the cubic symmetry. If we consider the average $\bar{J}^{\mu\nu}_{xx'} \equiv [J^{\mu\nu}_{xx'}]_J$ all couplings between pairs of orientations (μ', ν') which can be generated from (μ, ν) by cubic symmetry transformations have to be equal, i.e., $\bar{J}^{\mu\nu}_{xx'} = \bar{J}^{\mu'\nu'}_{xx'}$. As a consequence

$$\bar{J}^{\mu\nu}_{xx'} = J^{(0)}_{xx'}\delta^{\mu\nu} + J^{(1)}_{xx'}(1 - \delta^{\mu\nu}) \tag{8}$$

for models A and B, where all (μ, ν) with $\mu \neq \nu$ are connected by symmetry operations. For model C this is not the case. All pairs of face diagonals, which enclose an angle of $\pi/2$ [as, e.g., (1,1,0) and (1,−1,0)] are transformed among themselves. The same holds for face diagonals which enclose $\pi/3$ [like (1,1,0) and (0,1,1)]. Therefore $\bar{J}^{\mu\nu}_{xx'}$ can take on three different values, one of which can be absorbed in the definition of zero energy. We will number the face diagonals such that $|\mu - \nu| = 3$ implies an enclosed angle of $\pi/2$ [i.e., for (1,4), (2,5), and (3,6) pairs, see Fig. 1(c)]. Then

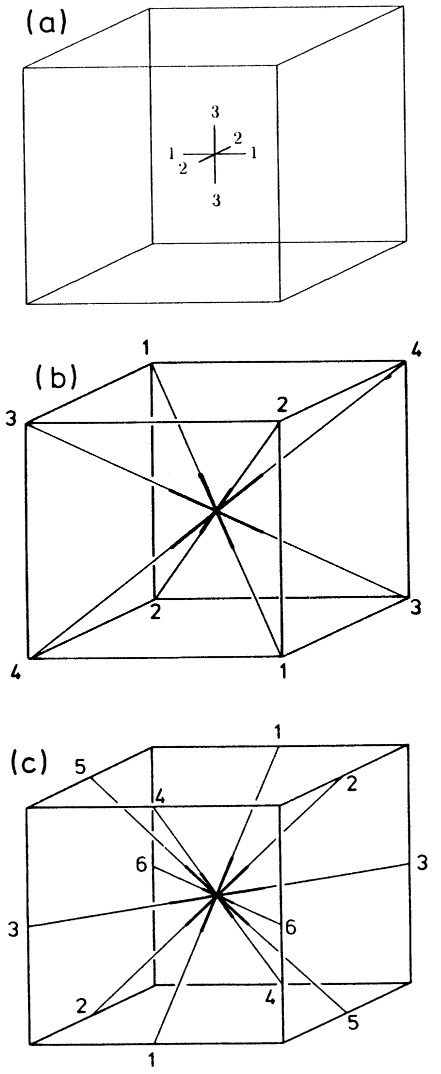

FIG. 1. In models A and B the orientable molecules align parallel to one of the three coordinate axes (A) or body diagonals (B) of the cube. In model C the local anisotropy causes the orientators to align parallel to the face diagonals.

$$\bar{\mathbf{J}}_{xx'} = \begin{pmatrix} J^{(0)}_{xx'} & 0 & 0 & J^{(1)}_{xx'} & 0 & 0 \\ 0 & J^{(0)}_{xx'} & 0 & 0 & J^{(1)}_{xx'} & 0 \\ 0 & 0 & J^{(0)}_{xx'} & 0 & 0 & J^{(1)}_{xx'} \\ J^{(1)}_{xx'} & 0 & 0 & J^{(0)}_{xx'} & 0 & 0 \\ 0 & J^{(1)}_{xx'} & 0 & 0 & J^{(0)}_{xx'} & 0 \\ 0 & 0 & J^{(1)}_{xx'} & 0 & 0 & J^{(0)}_{xx'} \end{pmatrix}. \tag{9}$$

For the above argument we implicitly assumed that the interaction $J^{\mu\nu}_{xx'}$ does only depend on the distance between x and x' but not on the orientation of the vector $x-x'$.

If the crystal medium including the defects remains cubic on the length scales of the coarse-grained effective Hamiltonian, the relations (8) and (9) will also hold for the realizations $J^{\mu\nu}_{xx'}$ of the random couplings. On the shortest length scales the structure of the medium deviates from that of a cubic crystal. There may be systems for which the contributions from these length scales lead to couplings with noncubic realizations. In this case cubic symmetry is restored only after averaging over the quenched fluctuations. For simplicity we will consider the first case in the main text. In Appendix A we construct and discuss some cubic ensembles which have noncubic realization.

The last step of our model building concerns a technical point. In the high-temperature phase the thermal averages $\langle n^\mu(x)\rangle$ of the $n^\mu(x)$ are equal to $1/p$ ($p=3$, 4, or 6 for models A, B, or C). For many purposes it is convenient to work with Potts variables[19,4]

$$s^\mu(x) = n^\mu(x) - \frac{1}{p} \tag{10}$$

so that $\langle s^\mu(x)\rangle = 0$ characterizes the orientationally disordered phase. In terms of these variables, the defect-defect interaction in Eq. (4) becomes

$$\tfrac{1}{2}\sum_{x,x'}\sum_{\mu\nu}^{p} J^{\mu\nu}_{xx'} s^\mu(x) s^\nu(x') + \sum_{x}\sum_{\mu} h(x) s^\mu(x) + \text{const}, \tag{11}$$

with $h(x) = (1/p)\sum_{x',\nu} J^{\mu\nu}_{xx'}$ independent of μ due to the cubic symmetry of the couplings. As $\sum_\mu s^\mu(x) = 0$ the random field term in Eq. (11) vanishes. A nonvanishing random field term will, however, be generated in the case of noncubic realizations. In this case the random field is strongly correlated with the random exchange (see Appendix A). The effect of random fields on the phase transitions will be discussed elsewhere.[20]

In terms of Potts spins our basic effective Hamiltonian is given by

$$H_{\text{eff}} = \sum_{x}\left\{\tfrac{1}{2}\epsilon(x)\mathbf{C}^0\epsilon(x) + \sum_{\mu}^{p} s^\mu(x)\tilde{\sigma}^\mu\epsilon(x)\right\} - \tfrac{1}{2}\sum_{x,x'}\sum_{\mu\nu}^{p} J^{\mu\nu}_{xx'} s^\mu(x) s^\nu(x'). \tag{12}$$

Equation (12) together with Eqs. (5)–(9) constitute the class of models which will be studied in the next sections.

In most theoretical approaches the defects are described by continuous variables, arising from a multipole expansion of the mass and charge distribution of the defect. In lowest order the defect—for example, the CN^- dumbbell—can be approximated by a sphere differing in radius from the replaced spherical atom.[9] If no dipole moment is present, the next term in the multipole expansion is the quadrupole moment.[3,8] Usually only one of the two terms is taken into account. In our model the defect is characterized by a discrete set of p states. In the high-temperature phase all states are equally occupied such that $\langle n^\mu(x)\rangle = 1/p$. This nonzero expectation value gives rise to a macroscopic dilatation as explained after Eq. (7) and to a random field as discussed after Eq. (11). Hence the replacement $n^\mu(x) \to 1/p$ corresponds to the approximation of the defect as a spherical dilatation centre. The deviations $s^\mu(x) = n^\mu(x) - 1/p$ specify preferred directions of the quadrupole in the limit of strong anisotropy, as explained in Ref. 4.

III. EXACT RELATIONS BETWEEN STRAIN AND DEFECT CORRELATION FUNCTION

Thermodynamic properties of the models introduced in the previous section can be obtained from the partition sum

$$Z = \int d^6\bar{\epsilon}\int\prod_x d^3u(x) \operatorname*{Tr}_{\{\vec{s}(x)\}} \exp\{-\beta H_{\text{eff}}\}, \tag{13}$$

where β denotes the inverse temperature and we have decomposed the strain fluctuations

$$\epsilon_{ij}(x) = \bar{\epsilon}_{ij} + \tilde{\epsilon}_{ij}(x) \tag{14}$$

into a homogeneous part $\bar{\epsilon}_{ij}$ and an inhomogeneous part $\tilde{\epsilon}_{ij}(x) = (\partial_i u_j + \partial_j u_i)/2$ which is related to displacements $\vec{u}(x)$ obeying natural boundary conditions at infinity [i.e., $\vec{u}(x) \to \mathbf{0}$ for $|x| \to \infty$]. The trace symbol stands for the sum over all orientational configurations of the defects. Quenched averages of thermal observables are obtained from the averaged free energy

$$F = -\beta^{-1}[\ln Z]. \tag{15}$$

Here and in the following $[\cdots]$ denotes the average over quenched disorder and $\langle\cdots\rangle$ denotes the average over thermal degrees of freedom, i.e., elastic deformations and orientational degrees of freedom. Note that the partition sum over strain fluctuations can be performed exactly as a sequence of Gaussian integrations. Due to this special feature of the models, all the strain correlation functions can be expressed by corresponding Potts spin (i.e., defect orientation) correlation functions.[8,21] In the subsequent sections we will make use of three exact relations which we now derive.

(i) From the identity

$$\int \mathcal{D}\epsilon \frac{\partial}{\partial \bar{\epsilon}_{ij}} \operatorname*{Tr}_{\{\vec{s}(x)\}} \exp\{-\beta H_{\text{eff}}\} = 0 \tag{16}$$

(where $\int \mathcal{D}\epsilon = \int d^6\bar{\epsilon} \int \prod_x d^3u(x)$) one gets

$$\sum_{kl} C^0_{ijkl} \, [\langle \bar{\epsilon}_{kl} \rangle] + \sum_{\mu} m^\mu \tilde{\sigma}^\mu_{ij} = 0. \tag{17}$$

Here $m^\mu \equiv N^{-1} \sum_x [\langle s^\mu(x) \rangle]$ is the average magnetization in the Potts spin system. $N = \sum_x 1$ is the system size. Thus we see that the "ferromagnetic," i.e., orientationally ordered phase is always accompanied by a homogeneous lattice deformation.

(ii) For the inhomogeneous part of the strain we get a similar relation if we replace $\partial/\partial\bar{\epsilon}_{ij}$ by $\delta/\delta u_i(x)$ in Eq. (16):

$$\sum_{kmn} \partial_k C^0_{ijkl} \langle \tilde{\epsilon}_{mn}(x) \rangle - \sum_k \sum_\mu \partial_k \langle s^\mu(x) \rangle \tilde{\sigma}^\mu_{ki} = 0. \tag{18}$$

The inhomogeneous displacements $\vec{u}(x)$ caused by the extra stresses of the defects can be obtained in explicit form if we introduce the lattice Green's function $G_{ij}(x)$ as the inverse of the differential operator $\sum_{kn} \partial_k \partial_n C^0_{lkmn} \equiv G^{-1}_{lm}(\partial)$.[14] Then we get from Eq. (18)

$$\langle u_i(x) \rangle = \sum_{x'} \sum_j G_{ij}(x - x') \sum_k \sum_\mu \frac{\partial}{\partial x'_k} \langle s^\mu(x') \rangle \tilde{\sigma}^\mu_{kj}. \tag{19}$$

A freezing of Potts spins into random directions such that $[\langle s^\mu(x) \rangle] = 0$ leads to randomly frozen inhomogeneous strains $\langle \tilde{\epsilon}_{ij} \rangle$ in the medium which vanish after quenched averaging $[\langle \tilde{\epsilon}_{ij} \rangle] = 0$.

(iii) Finally consider the elastic properties of the system. Due to the strain-defect coupling the bare elastic constants in $\mathbf{C}^0$ are renormalized to their observed values $\mathbf{C}$. The elastic compliance $\mathbf{S} = (\mathbf{C})^{-1}$ is defined as the matrix of second derivatives of the free energy with respect to an externally applied homogeneous stress. This leads to

$$S_{ijkl} = \beta N \, [\langle \bar{\epsilon}_{ij} \bar{\epsilon}_{kl} \rangle - \langle \bar{\epsilon}_{ij} \rangle \langle \bar{\epsilon}_{kl} \rangle] \equiv \beta N \langle \bar{\epsilon}_{ij} \bar{\epsilon}_{kl} \rangle_{\text{cum}}. \tag{20}$$

A simple shift of variables $\boldsymbol{\epsilon}' = \boldsymbol{\epsilon} + \mathbf{C}^0 \sum_{x\mu} s^\mu(x) \boldsymbol{\sigma}^\mu$ in the Gaussian integrations during the calculation of the strain cumulant results in the following identity:

$$\mathbf{S} = \mathbf{S}^0 + \frac{\beta}{N} \langle (\mathbf{S}^0 \boldsymbol{\sigma}_{\text{int}})^T \cdot (\mathbf{S}^0 \boldsymbol{\sigma}_{\text{int}}) \rangle_{\text{cum}}. \tag{21}$$

In this relation $\boldsymbol{\sigma}_{\text{int}}$ denotes the total extra stress due to the defects, i.e., $\boldsymbol{\sigma}_{\text{int}} = \sum_{x\mu} s^\mu(x) \boldsymbol{\sigma}^\mu$ and $\mathbf{S}^0 = (\mathbf{C}^0)^{-1}$ is the bare compliance matrix. Inserting the explicit form of $\boldsymbol{\sigma}_{\text{int}}$ leads to an exact relation between the Potts spin susceptibility

$$\chi^{\mu\nu}(x, x') \equiv \beta \langle s^\mu(x) s^\nu(x') \rangle_{\text{cum}} \tag{22}$$

and the elastic compliance

$$\mathbf{S} = \mathbf{S}^0 + \sum_{\mu\nu} (\mathbf{S}^0 \tilde{\boldsymbol{\sigma}}^\mu)^T \chi^{\mu\nu} (\mathbf{S}^0 \tilde{\boldsymbol{\sigma}}^\nu), \tag{23}$$

where $\chi^{\mu\nu} = N^{-1} \sum_{x,x'} \chi^{\mu\nu}(x, x')$.

IV. PHASE DIAGRAM

In this section we are going to calculate the phase diagram of the orientational degrees of freedom coupled to elastic distortions. Some of the results of this and the following section have previously been published in Ref. 4.

We concentrate here on models A and B, whereas model C will be discussed in a separate section (6). For models A and B it is convenient to use a different representation of Potts spins.[4] For $p = 3$ only the diagonal elements of $\tilde{\boldsymbol{\sigma}}^\mu$ are nonvanishing. They can be represented as three-dimensional vectors $\vec{\sigma}^\mu = (\tilde{\sigma}^\mu_{11}, \tilde{\sigma}^\mu_{22}, \tilde{\sigma}^\mu_{33})$. These three vectors $\{\vec{\sigma}^\mu\}$ ($\mu = 1, 2, 3$) constitute a three-dimensional Potts basis $\vec{e}^{\,\mu} = (\sqrt{3}/\sigma)\vec{\sigma}^\mu$, because $\sum_\mu \vec{\sigma}^\mu = \sum_\mu \tilde{\boldsymbol{\sigma}}^\mu = 0$. Explicitly the Cartesian components of these Potts vectors read

$$\{\vec{e}^{\,1}, \vec{e}^{\,2}, \vec{e}^{\,3}\} = \left\{ \frac{1}{\sqrt{3}} \begin{pmatrix} 2 \\ -1 \\ -1 \end{pmatrix}, \frac{1}{\sqrt{3}} \begin{pmatrix} -1 \\ 2 \\ -1 \end{pmatrix}, \frac{1}{\sqrt{3}} \begin{pmatrix} -1 \\ -1 \\ 2 \end{pmatrix} \right\}. \tag{24}$$

For p=4 only the off-diagonal elements of $\tilde{\boldsymbol{\sigma}}^\mu$ are nonvanishing. They are represented as vectors $\vec{\sigma}^\mu = (\tilde{\sigma}^\mu_{23}, \tilde{\sigma}^\mu_{31}, \tilde{\sigma}^\mu_{12})$, so that the corresponding three-dimensional Potts basis $\vec{e}^{\,\mu} = (\sqrt{4}/\sigma)\vec{\sigma}^\mu$ reads

$$\{\vec{e}^{\,1}, \vec{e}^{\,2}, \vec{e}^{\,3}, \vec{e}^{\,4}\} = \left\{ \begin{pmatrix} 1 \\ -1 \\ -1 \end{pmatrix}, \begin{pmatrix} -1 \\ 1 \\ -1 \end{pmatrix}, \begin{pmatrix} -1 \\ -1 \\ 1 \end{pmatrix}, \begin{pmatrix} 1 \\ 1 \\ 1 \end{pmatrix} \right\}. \tag{25}$$

The effective Hamiltonian may be rewritten in terms of Potts spins $\vec{s}(x) \in \{\vec{e}^{\,\mu}\}$, which can be one of the above basis vectors

$$H_{\text{eff}} = \tfrac{1}{2} \sum_x \epsilon(x) \mathbf{C}^0 \epsilon(x) + \sum_x \sum_{i,j,k} s_i(x) K_{ijk} \epsilon_{jk}(x) - \tfrac{1}{2} \sum_{x,x'} J_{xx'} \vec{s}(x) \cdot \vec{s}(x') \tag{26}$$

with $K_{ijk} = \sigma/\sqrt{3}$ for $i = j = k$ (and zero otherwise) in model A and $K_{ijk} = \sigma/2$ for $i \neq j \neq k \neq i$ (and zero otherwise) in model B.

In order to solve the model as defined in Eq. (26) we are going to introduce two major approximations.

(a) The interaction between the Potts spins will be taken as infinite ranged. The couplings $J_{xx'}$ are uncorrelated Gaussian variables with mean

$$[J_{xx'}] = \frac{J_0}{N} \tag{27}$$

and variance

$$[(J_{xx'} - [J_{xx'}])^2] = \frac{J^2}{N}. \tag{28}$$

J_0 and J^2 are coupling constants of a coarse-grained model and therefore they cannot be determined directly from experiments. In the following they are treated as adjustable parameters.

(b) The homogeneous deformations $\bar{\epsilon}$ are treated exactly, whereas fluctuations in the strain field $\tilde{\epsilon}_{ij}(x)$ are treated in a self-consistent cumulant expansion.

Given these approximations, the phase diagram can be calculated explicitly, in particular the transition temperatures and order parameters for the glassy phase and the long-ranged ordered phase. These calculations are the central point of Sec. IV.

In order to take the configurational average over $J_{xx'}$ before the thermal average, we use the replica trick[2]

$$[\ln Z] = \lim_{n\to 0} \frac{[Z^n]-1}{n} \tag{29}$$

with

$$\begin{aligned}[Z^n] &= \int \mathcal{D}\epsilon \operatorname*{Tr}_{\{\vec{s}^{\,\alpha}(x)\}} [\exp(-\beta H_{\text{eff}}\{\vec{u}^{\alpha}(x),\vec{s}^{\,\alpha}(x)\})] \\ &= \int \mathcal{D}\epsilon \operatorname*{Tr}_{\{\vec{s}^{\,\alpha}(x)\}} \exp\left\{+\frac{J^2}{2N}\sum_{\alpha<\beta}\sum_{ij}\left(\sum_x s_i^{\alpha}(x)s_j^{\beta}(x)\right)^2 - \frac{\hat{J}_0}{2N}\sum_{\alpha}\sum_{i}\left(\sum_x s_i^{\alpha}(x)\right)^2\right. \\ &\qquad \left. -\frac{1}{2}\sum_x\sum_{\alpha}\sum_{ijk} s_i^{\alpha}(x)K_{ijk}\epsilon_{jk}^{\alpha}(x) - \frac{1}{2}\sum_x\sum_{\alpha}\sum_{ijkl}\epsilon_{ij}^{\alpha}(x)C_{ijkl}^{0}\epsilon_{kl}^{\alpha}(x)\right\}. \end{aligned} \tag{30}$$

Here we put $\beta = 1/k_BT \equiv 1$ and $\hat{J}_0 \equiv J_0 + (p-2)J^2$. (The temperature dependence of the system can easily be recovered at the end of the calculation by multiplying each of the constants J_0, J, $\hat{J}_0$, K, and C^0 with β.) In a Potts model without coupling to strains even an antiferromagnetic average of bonds ($J_0 < 0$) can give rise to ferromagnetic and glassy states due to the renormalization of the coupling. For Potts models with $p \geq 4$ a transition to a glassy state can only be reached for $J_0 < 0$.[19] Additive constants in the exponent have been dropped. Gauss transformation yields

$$\begin{aligned}[Z^n] &= \int \mathcal{D}\{Q,M\}\exp\left\{-\frac{J^2N}{2}\sum_{\alpha<\beta}\sum_{ij}(Q_{ij}^{\alpha\beta})^2 - \frac{\hat{J}_0N}{2}\sum_{\alpha}\sum_{i}(M_i^{\alpha})^2\right\} \\ &\quad \times \int \mathcal{D}\epsilon\exp\left\{-\tfrac{1}{2}\sum_x\sum_{\alpha}\sum_{ijkl}\epsilon_{ij}^{\alpha}(x)C_{ijkl}^{0}\epsilon_{kl}^{\alpha}(x) + \sum_x \ln z(x)\right\}, \end{aligned} \tag{31}$$

where $z(x)$ is the single-spin partition function with an x-dependent field $\epsilon_{ij}(x)$:

$$z(x) = \operatorname*{Tr}_{\{\vec{s}^{\,\alpha}\}} \exp\left\{J^2\sum_{\alpha<\beta}\sum_{ij}s_i^{\alpha}Q_{ij}^{\alpha\beta}s_j^{\beta} + \hat{J}_0\sum_{\alpha}\sum_{i}s_i^{\alpha}M_i^{\alpha} - \sum_{\alpha}\sum_{ijk}s_i^{\alpha}K_{ijk}\epsilon_{jk}^{\alpha}(x)\right\} \tag{32}$$

and

$$\mathcal{D}\{Q,M\} = \prod_{\alpha<\beta}^{n}\prod_{ij}^{3}\left[dQ_{ij}^{\alpha\beta}\left(\frac{NJ^2}{2\pi}\right)^{1/2}\right]\prod_{\alpha}^{n}\prod_{i}^{3}\left[dM_i^{\alpha}\left(\frac{N\hat{J}_0}{2\pi}\right)^{1/2}\right]. \tag{33}$$

The strain field $\epsilon_{ij}^{\alpha}(x)$ is decomposed into a homogeneous $\bar{\epsilon}_{ij}^{\alpha}$ and an inhomogeneous part $\tilde{\epsilon}_{ij}^{\alpha}(x) = \epsilon_{ij}^{\alpha}(x) - \bar{\epsilon}_{ij}^{\alpha}$.[22,23] The partition function of a single spin at site x can be decomposed accordingly

$$z(x) = z_0\left\langle \exp - \sum_{\alpha}\sum_{ijk}s_i^{\alpha}K_{ijk}\tilde{\epsilon}_{jk}^{\alpha}(x)\right\rangle_0, \tag{34}$$

where the thermal average $\langle\cdots\rangle_0$ has to be evaluated with z_0

$$z_0 = \operatorname*{Tr}_{\{\vec{s}^{\,\alpha}\}} \exp\left\{J^2\sum_{\alpha<\beta}\sum_{ij}s_i^{\alpha}Q_{ij}^{\alpha\beta}s_j^{\beta} + \hat{J}_0\sum_{\alpha}\sum_{i}s_i^{\alpha}M_i^{\alpha} - \sum_{\alpha}\sum_{ijk}s_i^{\alpha}K_{ijk}\bar{\epsilon}_{jk}^{\alpha}\right\}. \tag{35}$$

(a) In a first approximation we are going to ignore inhomogeneous strain fluctuations, so that the averaged partition function reads

$$[Z^n] = \int \mathcal{D}\{Q, M, \bar{\epsilon}\} e^{-N f_0\{Q,M,\bar{\epsilon}\}} \tag{36}$$

with

$$f_0\{Q, M, \bar{\epsilon}\} = \frac{J^2}{2} \sum_{\alpha<\beta} \sum_{ij} (Q_{ij}^{\alpha\beta})^2 + \frac{\hat{J}_0}{2} \sum_{\alpha} \sum_{i} (M_i^\alpha)^2 + \tfrac{1}{2} \sum_{\alpha} \sum_{ijkl} \bar{\epsilon}_{ij}^\alpha C_{ijkl}^0 \bar{\epsilon}_{kl}^\alpha - \ln z_0. \tag{37}$$

In the thermodynamic limit all integrations can be done by saddle-point methods, yielding

$$Q_{ij}^{\alpha\beta} = \langle s_i^\alpha s_j^\beta \rangle_0, \tag{38}$$

$$C_{ijkl}^0 \bar{\epsilon}_{kl}^\alpha = -K_{kij} \langle s_k^\alpha \rangle_0 = -K_{kij} M_k^\alpha . \tag{39}$$

We look for a replica symmetric saddle point

$$Q_{ij}^{\alpha\beta} = Q_{ij}, \quad M_i^\alpha = M_i, \quad \bar{\epsilon}_{ij}^\alpha = \bar{\epsilon}_{ij} . \tag{40}$$

The single-spin partition function can then be evaluated by introducing a Gaussian noise source y_i with variance $[y_i y_j]_{\vec{y}} = Q_{ij}$

$$\ln z_0 = n[\ln z_1]_{\vec{y}} \tag{41}$$

with

$$z_1 = \operatorname*{Tr}_{\{\vec{s}\}} \exp\left\{ J\vec{y} \cdot \vec{s} - \frac{J^2}{2} \sum_{ij} Q_{ij} s_i s_j + \sum_{ij} s_i (\hat{J}_0 \mathbf{1} + \mathbf{K}^T \mathbf{S}^0 \mathbf{K})_{ij} M_j \right\}. \tag{42}$$

We make the following ansatz for the order parameter:

$$m^\mu = \vec{e}^{\,\mu} \cdot \vec{M} = M I_{\mu 1} \tag{43}$$

and

$$q^{\mu\nu} = \vec{e}^{\,\mu} \cdot \mathbf{Q} \cdot \vec{e}^{\,\nu} = \frac{q_L - q_T}{p-1} I_{\mu 1} I_{\nu 1} + q_T I_{\mu\nu}, \tag{44}$$

where $I_{\mu\nu} \equiv \vec{e}^{\,\mu} \cdot \vec{e}^{\,\nu} = p\delta_{\mu\nu} - 1$. With the basis of Eq. (24) this implies for $p = 3$

$$M_i = M e_i^1 = \left(M/\sqrt{3} \right) I_{i1}, \tag{45}$$

$$3Q_{ij} = \frac{q_L - q_T}{2} I_{i1} I_{j1} + q_T I_{ij} . \tag{46}$$

Then the model of Eqs. (36) and (37) is identical to the isotropic Potts model without coupling to the elastic degrees of freedom,[19,24] if we define an effective ferromagnetic coupling constant

$$\hat{J}_{\text{eff}} = \hat{J}_0 + \frac{\sigma^2}{3} (S_{1111}^0 - S_{1122}^0). \tag{47}$$

For $p = 4$ the order parameters in real space are given by

$$M_i = M e_i^1, \quad Q_{ij} = \frac{q_L - q_T}{3} e_i^1 e_j^1 + q_T \delta_{ij} . \tag{48}$$

Hence the effective coupling constant is

$$\hat{J}_{\text{eff}} = \hat{J}_0 + \frac{\sigma^2}{4} S_{1212}^0 . \tag{49}$$

The random part of the interaction is not affected by the uniform displacement.

To conclude: The model of orientational degrees of freedom with cubic anisotropy coupled to uniform lattice distortions has the same phase diagram as the isotropic Potts model[19,24] (see Fig. 2) without coupling to the elastic degrees of freedom, provided the renormalization of the ferromagnetic coupling constant is taken into account.

(b) What is the effect of fluctuations in the strain field $\tilde{\epsilon}_{ij}^\alpha(x) = \epsilon_{ij}^\alpha(x) - \bar{\epsilon}_{ij}^\alpha$? We assume that these fluctuations are small, so that a second-order cumulant expansion is applicable. The validity of this assumption will be discussed at the end of this section. The expansion for $z(x)$ reads explicitly

$$z(x) = z_0 \exp\left\{ \tfrac{1}{2} \sum_{\alpha\beta} \sum_{ijklrs} K_{ijk} K_{lrs} F_{il}^{\alpha\beta} \tilde{\epsilon}_{jk}^\alpha(x) \tilde{\epsilon}_{rs}^\beta(x) \right\} \tag{50}$$

with

$$F_{il}^{\alpha\beta} = \langle s_i^\alpha s_l^\beta \rangle_0 - \langle s_i^\alpha \rangle_0 \langle s_l^\beta \rangle_0 . \tag{51}$$

The thermal averages $\langle \cdots \rangle_0$ have to be calculated with z_0 and $z(x)$ depends on Q and M through $F_{il}^{\alpha\beta}$. To discuss the phase diagram of the orientational degrees of freedom we integrate out the inhomogeneous strain field

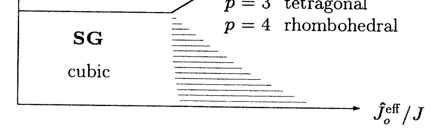

FIG. 2. Phase diagram of models A ($p = 3$) and B ($p = 4$). In the high-temperature phase (PM) and in the pure glass phase (SG) $\mathbf{m} = 0$ and the lattice is cubic. In the uniform ordered phase (FM) $\mathbf{m} = m\mathbf{e}^1$ and the lattice is tetragonal ($p = 3$) or rhombohedral ($p = 4$).

$$z^{(\mathrm{inh})}\{Q,M\} = \int \prod_x d^3u(x) \exp\left\{ -\tfrac{1}{2} \sum_x \sum_{\alpha\beta} \sum_{ijkl} \tilde{\epsilon}_{ij}^{\alpha}(x)\tilde{\epsilon}_{kl}^{\beta}(x) \left(\delta^{\alpha\beta} C_{ijkl}^{0} - \sum_{rs} F_{rs}^{\alpha\beta} K_{rij} K_{skl} \right) \right\} \tag{52}$$

so that we are left with an effective free energy as a functional of Q, M, and $\bar{\epsilon}$:

$$[Z^n] = \int \mathcal{D}\{Q,M,\bar{\epsilon}\} \exp\left\{ -N f_0\{Q,M,\bar{\epsilon}\} + \ln z^{(\mathrm{inh})}\{Q,M\} \right\}. \tag{53}$$

The remaining integrals can be evaluated by saddle-point methods. We assume a replica symmetric solution (40) and find

$$\begin{aligned}\hat{J}_0(M_i - \langle s_i^{\alpha}\rangle_0) &= \frac{\partial}{\partial M_i}\frac{1}{N}\lim_{n\to 0}\left(\frac{1}{n}\ln z^{(\mathrm{inh})}\right) \\ &= K_{jkl}K_{trs}\langle s_j^{\alpha}\rangle_0 \frac{\partial}{\partial M_i}\langle s_t^{\alpha}\rangle_0 \sum_x \left(\langle \tilde{\epsilon}_{kl}(x)\tilde{\epsilon}_{rs}(x)\rangle - \langle \tilde{\epsilon}_{kl}(x)\rangle\langle \tilde{\epsilon}_{rs}(x)\rangle \right),\end{aligned} \tag{54}$$

$$J^2(Q_{ij} - \langle s_i^{\alpha} s_i^{\beta}\rangle_0) = \frac{\partial}{\partial Q_{ij}}\frac{1}{N}\lim_{n\to 0}\left(\frac{1}{n}\ln z^{(\mathrm{inh})}\right) = K_{ukl}K_{trs}\frac{\partial}{\partial Q_{ij}}\langle s_u^{\alpha} s_t^{\beta}\rangle_0 \frac{1}{N}\sum_x \langle \tilde{\epsilon}_{kl}(x)\rangle\langle \tilde{\epsilon}_{rs}(x)\rangle, \tag{55}$$

and

$$C_{ijkl}^{0}\bar{\epsilon}_{kl} = -K_{kij}\langle s_k^{\alpha}\rangle_0. \tag{56}$$

These equations determine the phase diagram and the order parameters M and Q, once the correlations of $\tilde{\epsilon}(x)$ and $\bar{\epsilon}$ have been calculated in terms of M and Q.

This can be done perturbatively in a Ginzburg-Landau expansion in Q and M. To study the transition from the paramagnetic phase to the collinear ferromagnet we assume $q_T = 0, M \neq 0$, and $q_L \neq 0$. The detailed calculations are presented in Appendix B. The result is

$$\begin{aligned}M(1-\beta\hat{J}_{\mathrm{eff}}) = {}& \frac{M^2}{2}\beta^2\hat{J}_{\mathrm{eff}}^2 - \frac{\beta^3\hat{J}_0 M}{p-1}\left(1+(p-2)\frac{3}{2}M\beta\hat{J}_0\right) K_{rij}K_{skl}e_r^1 e_s^1 \frac{1}{N}\sum_x [\langle \tilde{\epsilon}_{ij}(x)\tilde{\epsilon}_{kl}(x)\rangle] \\ &+ O(M^3, Q^2, MQ).\end{aligned} \tag{57}$$

The paramagnetic solution $M = 0$ becomes unstable to ferromagnetic fluctuations at the critical temperature

$$\frac{T_F}{\hat{J}_0} = 1 + \frac{\sigma^2}{3\hat{J}_0}(S_{1111}^0 - S_{1122}^0) - \frac{\sigma^2}{6\hat{J}_0^2}\frac{1}{N}\sum_x\sum_{ij}[\langle \tilde{\epsilon}_{ii}(x)\tilde{\epsilon}_{jj}(x)\rangle] e_i^1 e_j^1 \tag{58}$$

for $p = 3$ and

$$\frac{T_F}{\hat{J}_0} = 1 + \frac{\sigma^2}{4\hat{J}_0}S_{1212}^0 - \frac{2\sigma^2}{3\hat{J}_0^2}\frac{1}{N}\sum_x [\langle \tilde{\epsilon}_{23}(x)\rangle\langle \tilde{\epsilon}_{23}(x)\rangle + \langle \tilde{\epsilon}_{31}(x)\rangle\langle \tilde{\epsilon}_{31}(x)\rangle + \langle \tilde{\epsilon}_{12}(x)\rangle\langle \tilde{\epsilon}_{12}(x)\rangle] \tag{59}$$

for $p = 4$. The transition is in general first order. Without fluctuations $\tilde{\epsilon} = 0$ the coefficient of the cubic term M^3 in $f\{Q,M,\bar{\epsilon}\}$ is the same as in Ref. 19,

$$M(1-\beta\hat{J}_{\mathrm{eff}}) = \frac{M^2}{2}\beta^2\hat{J}_{\mathrm{eff}}^2 + O(M^3, Q^2, MQ) \tag{60}$$

with $\hat{J}_0$ replaced by $\hat{J}_{\mathrm{eff}}$. Fluctuations $\tilde{\epsilon} \neq 0$ tend to reduce the cubic term, i.e., weaken the first-order transition. Since the transition to the ferromagnetic phase is discontinuous, the expansion of Eq. (57) is not really justified. Nevertheless we expect it to give a qualitative picture of the correct phase diagram, as contained in Eqs. (58) and (59).

To discuss the transition from the paramagnetic to the spin-glass phase we assume $q_L = q_T = q$ and $M = 0$. As noted in Refs. 19 and 24 the transition is continuous for $p = 3$ and 4. This remains to be true in our model at least for small coupling constant σ, where the cumulant expansion is justified. To calculate the change in the critical temperature T_G, we just need to know

$$\langle s_i^{\alpha} s_j^{\beta}\rangle_0 = J^2 Q_{ij} + O(q^2) \tag{61}$$

to lowest order in q. For the three-state model the transition temperature is given by

$$\begin{aligned}\left(\frac{T_G}{J}\right)^2 = 1 &+ \left(\frac{\sigma}{3J}\right)^2 \lim_{q\to 0}\frac{1}{q}\frac{1}{N} \\ &\times \sum_x\sum_{ij} I_{ij}[\langle \tilde{\epsilon}_{ii}(x)\rangle\langle \tilde{\epsilon}_{jj}(x)\rangle].\end{aligned} \tag{62}$$

The time persistent correlation, $q \neq 0$, gives rise to a random static strain $\langle \tilde{\epsilon}_{ii}(x)\rangle \neq 0$, which averages to zero $(1/N)\sum_x[\langle \tilde{\epsilon}_{ii}(x)\rangle] = 0$, but has a nonzero variance proportional to Q_{ij}. Hence the last term in Eq. (62) goes to a finite limit as $q \to 0$. For the four-state model the corresponding equation reads

$$\left(\frac{T_G}{J}\right)^2 = 1 + \frac{1}{3}\left(\frac{\sigma}{J}\right)^2 \lim_{q\to 0}\frac{1}{q}\frac{1}{N}\sum_x [\langle\tilde{\epsilon}_{23}(x)\rangle\langle\tilde{\epsilon}_{23}(x)\rangle + \langle\tilde{\epsilon}_{31}(x)\rangle\langle\tilde{\epsilon}_{31}(x)\rangle + \langle\tilde{\epsilon}_{12}(x)\rangle\langle\tilde{\epsilon}_{12}(x)\rangle]. \tag{63}$$

The critical temperature is higher than in a model without coupling to the elastic strain, which means that the random interaction between the quadrupoles is enhanced by nonuniform lattice deformations. This effect can only be seen in a self-consistent cumulant expansion, as defined in Eqs. (50)–(52). Straightforward second-order perturbation theory in σ would produce no shift in T_G because to lowest order in σ, we have $\langle\tilde{\epsilon}_{ij}(x)\rangle = 0$.

The cumulant expansion is useful only if two requirements are fulfilled.

(a) The coupling between the elastic strain and the orientational degrees of freedom is small compared to the other coupling constants, i.e., $\sigma/T < 1$. For the ferromagnetic transition this implies $\sigma/\hat{J}_0 < 1$ [see Eqs. (58) and (59)] and for the glass transition $\sigma/J < 1$ [see Eqs. (62) and (63)].

(b) The inhomogeneous strain fluctuations are small or at least finite. Since the "stiffness" for the inhomogeneous strain is renormalized by local spin correlations only [see Eqs. (50)–(52)], we expect these fluctuations to remain finite — even close to the ferromagnetic transition, where nonlocal spin correlations become long ranged. In this sense our theory is at least consistent.

So far we have only discussed the replica symmetric solution of the saddle-point equations. It is well known that this solution is unstable in the spin-glass phase.[24] The correct mean-field solution requires replica symmetry breaking and shows a rich structure in the low-temperature phase. Here we have focused on the overall phase diagram. The transition lines from the high-temperature phase and the crystal symmetry in the low-temperature phase are not expected to depend on the assumption of replica symmetry. However it would be interesting to study the correct mean-field solution in the glassy phase, in order to discuss the dynamics and the quasielastic peak in the low-temperature phase as well as possible transitions between various low-temperature phases. This has not been attempted so far.

V. ELASTIC PROPERTIES

In this section we are going to discuss the modification of the elastic properties due to long-range orientational order or random freezing of the quadrupoles. The first part of our discussion will be put in the context of mean-field theory, as discussed in the previous section. We then go on to discuss which of these results are expected to survive in a short-range model.

A. Homogeneous deformations

Long-range orientational order causes a macroscopic distortion of the lattice (see Fig. 2). The exact relation [Eq. (17)] coincides with the saddle-point equation with **M** calculated in mean-field theory. The long-range ordered phase is characterized by a nonzero magnetization $M_i = Me_i^1$, which gives rise to a tetragonal displacement for $p = 3$

$$\bar{\epsilon}_{ij} = -\delta_{ij}e_i^1\frac{\sigma}{\sqrt{3}}M(S^0_{1111} - S^0_{1122}) \tag{64}$$

and a rhombohedral displacement for $p = 4$

$$\bar{\epsilon}_{ij} = -(1-\delta_{ij})\frac{\sigma}{2}MS^0_{1212}. \tag{65}$$

As discussed in the previous section, the distortive phase transition is discontinuous in both cases.

B. Elastic constants

In Sec. III we derived an exact relation between the elastic compliance and the uniform susceptibility

$$\mathbf{S} = \mathbf{S}^0 + \mathbf{S}^0\mathbf{K}\chi\mathbf{K}^T(\mathbf{S}^0)^T. \tag{66}$$

Obviously this relation also holds for the long-range model, where the ferromagnetic susceptibility has to be calculated in mean-field approximation. This is most easily done by applying a uniform field **h** and calculating the response $\chi_{ij} = dM_i/dh_j|_{\mathbf{h}} = 0$. Two simple cases will be discussed in detail.

(a) The ferromagnetic model without random interactions and without nonuniform strain fluctuations. In this case the uniform susceptibility is simply related to the local susceptibility via

$$\chi_{ij} - \chi_{ik}^{\text{loc}}\chi_{kj}\hat{J}_{\text{eff}} = \chi_{ij}^{\text{loc}} \tag{67}$$

and the local susceptibility is given by

$$\chi_{ij}^{\text{loc}} = \frac{\operatorname*{Tr}_{\{\vec{s}\}} \; s_i s_j \exp\{\beta\hat{J}_{\text{eff}}\vec{M}\cdot\vec{s}\}}{\operatorname*{Tr}_{\{\vec{s}\}} \; \exp\{\beta J_{\text{eff}}\vec{M}\cdot\vec{s}\}} - M_iM_j. \tag{68}$$

The local susceptibility can be expressed in terms of $M_i = Me_i^1$ as follows[19]:

$$\chi_{\text{loc}}^{\mu\nu} = \sum_{ij} e_i^\mu\chi_{ij}^{\text{loc}}e_j^\nu = \beta(1-M)(MI_{\mu 1}I_{\nu 1} + I_{\mu\nu}). \tag{69}$$

Potts symmetry requires the same structure for $\chi^{\mu\nu}$

$$\chi^{\mu\nu} = \sum_{ij} e_i^\mu\chi_{ij}e_j^\nu = \frac{\chi_L - \chi_T}{(p-1)}I_{\mu 1}I_{\nu 1} + \chi_T I_{\mu\nu} \tag{70}$$

with

$$\chi_{ij} = \frac{\chi_L - \chi_T}{6}I_{i1}I_{j1} + \frac{\chi_T}{3}I_{ij} \quad \text{for} \quad p = 3 \tag{71}$$

and

$$\chi_{ij} = \frac{\chi_L - \chi_T}{3} e_i^1 e_j^1 + \chi_T \delta_{ij} \quad \text{for} \quad p = 4. \tag{72}$$

The matrix equation for χ_{ij} is then easily solved:

$$\chi_T = \frac{\beta(1-M)}{1 - \beta \hat{J}_{\text{eff}}(1-M)}, \qquad \chi_L = \frac{\beta(1-M)(1+(p-1)M)}{1 - \beta \hat{J}_{\text{eff}}(1-M)(1+(p-1)M)}. \tag{73}$$

For high temperatures $\chi_L = \chi_T = \chi = (T - T_F)^{-1}$ the susceptibility shows Curie-Weiss behavior. The divergence at T_F is cut off by the discontinuous transition at $T_c > T_F$. The mean-field equation of the homogeneous Potts system $(\partial/\partial M) f(M, \beta) = 0$ can be solved analytically for $\beta(M)$. At

$$T_c = \frac{\hat{J}_{\text{eff}}}{2} \frac{p-2}{p-1} \frac{p^2}{\ln(p-1)}$$

the free energy of the paramagnetic and the ferromagnetic phases are equal. In Fig. 3 we show the uniform susceptibility as a function of temperature for a particular set of parameters. For $p = 3$ the elastic compliance above T_c is given by

$$S_{ijkl} = S^0_{ijkl} + \left(\frac{\sigma}{3}\right)^2 \chi S^0_{ijrr} I_{rs} S^0_{sskl}. \tag{74}$$

Hence there is no modification of the shear compliance S^0_{1212}, an increase in

$$S_{1111} = S^0_{1111} + 2\left(\frac{\sigma}{3}\right)^2 \chi (S^0_{1111} - S^0_{1122})^2 \tag{75}$$

and a corresponding decrease of

$$S_{1122} = S^0_{1122} - 2\left(\frac{\sigma}{3}\right)^2 \chi (S^0_{1111} - S^0_{1122})^2, \tag{76}$$

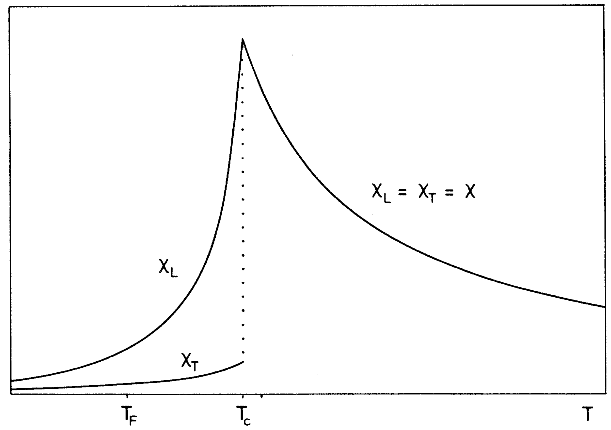

FIG. 3. Susceptibility of the homogeneous $p = 3$ Potts model. The high-temperature branch diverges at T_F, the two low-temperature branches diverge at the temperature marked above T_c. The divergences are cut off at T_c by the first-order transition.

such that $S_{1111} + S_{1122} = \text{const}$.

Below T_c the elastic compliance is that of a tetragonal lattice. In the weak-coupling expansion the elastic constants are given by

$$\begin{aligned} C_{1111} &= C^0_{1111} - \left(\frac{\sigma}{3}\right)^2 2\chi_L, \\ C_{1122} &= C^0_{1122} - \left(\frac{\sigma}{3}\right)^2 \chi_L, \\ C_{2222} &= C^0_{1111} - \left(\frac{\sigma}{3}\right)^2 \frac{\chi_L + 3\chi_T}{2}, \\ C_{2233} &= C^0_{1122} - \left(\frac{\sigma}{3}\right)^2 \frac{\chi_L - 3\chi_T}{2}. \end{aligned} \tag{77}$$

For $p = 4$ the elastic compliance above T_c is given by

$$S_{1212} = S^0_{1212}(1 + \sigma^2 \chi S^0_{1212}) \tag{78}$$

and no modification of the other elastic constants, i.e., $S_{1111} = S^0_{1111}$ and $S_{1122} = S^0_{1122}$. Below T_c the elastic constants are those of a rhombohedral lattice. In the weak-coupling expansion they are given by

$$\begin{aligned} C_{1212} &= C^0_{1212} - \left(\frac{\sigma}{2}\right)^2 \frac{\chi_L + 2\chi_T}{3} = C_{3131} = C_{2323}, \\ C_{1223} &= -\left(\frac{\sigma}{2}\right)^2 \frac{\chi_L - \chi_T}{3} = C_{2313} = -C_{1213}, \end{aligned} \tag{79}$$

and $C_{1111} = C^0_{1111}, C_{1122} = C^0_{1122}$. In Fig. 4 the elastic constants C_{1212} and C_{1213} are shown as functions of the temperature.

(b) The glassy regime without ferromagnetic coupling, $\hat{J}_{\text{eff}} = 0$. In this case we expect the uniform susceptibility to be identical to the local one $\chi_{ij} = \chi^{\text{loc}}_{ij}$ with

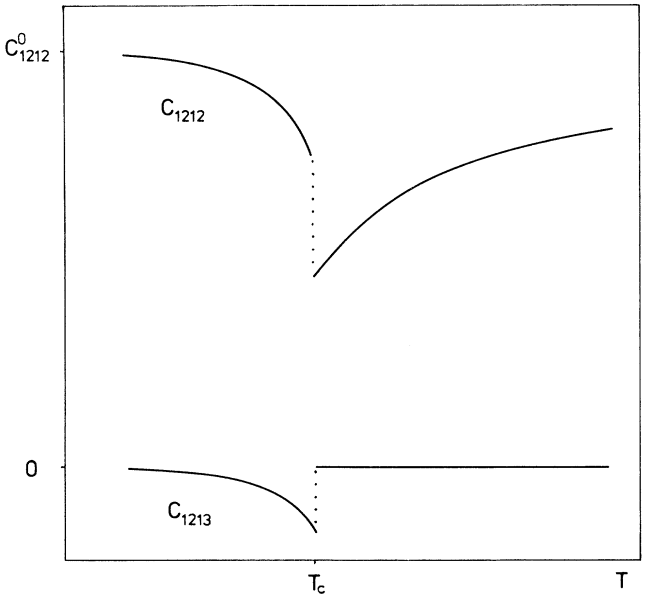

FIG. 4. C_{1212} and C_{1213} for model B at the ferroelastic transition. The system is cubic above T_c and rhombohedral below T_c.

$$\chi_{ij}^{\rm loc} = \frac{1}{T}\frac{1-q}{3} I_{ij} \quad \text{for} \quad p = 3 \tag{80}$$

and

$$\chi_{ij}^{\rm loc} = \frac{1}{T}\frac{1-q}{4} \delta_{ij} \quad \text{for} \quad p = 4. \tag{81}$$

Hence the uniform susceptibility is predicted to show Curie behavior $\chi \sim 1/T$ above T_G and a cusplike singularity at T_G. The elastic constants are modified accordingly as shown in Fig. 5. Again, symmetry determines which of the elastic constants are affected by the random freezing of the quadrupoles: S_{1212} for $p = 4$, S_{1111} and S_{1122} for $p = 3$. The tensor of elastic constants always has cubic symmetry—even below T_G.

C. Nonuniform strain fluctuations

The random part of the interaction $J \neq 0$ between the quadrupoles gives rise to a freezing of the orientations in random directions. Randomly frozen in quadrupoles cause a local, static distortion of the lattice. This effect is most important for the glassy phase. Hence we discuss it in detail for $M = \bar{\epsilon} = 0$.

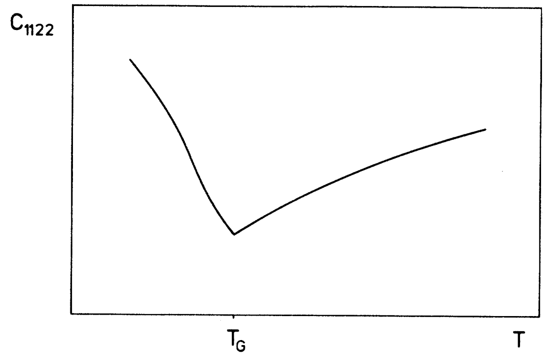

FIG. 5. C_{1122} for model A at the glass transition. Below T_G the elastic constant increases due to the stochastic freezing of orientations.

The glassy phase is characterized by a nonzero order parameter Q_{ij}, which for $p = 3$ has the simple structure $Q_{ij} = (q/3)I_{ij}$. Within our second-order cumulant expansion the fluctuations in the strain field contribute to the partition functions as follows:

$$z^{\rm inh}(q) = \int \mathcal{D}\epsilon \exp\left\{ -\frac{1}{2} \sum_x \sum_\alpha \sum_{ijkl} \tilde{\epsilon}_{ij}^{\alpha}(x)\tilde{\epsilon}_{kl}^{\alpha}(x) \left(C_{ijkl}^0 - \frac{1-q^0}{3}\delta_{ij}\delta_{kl}I_{ik} \right) + \frac{1}{2} \sum_x \sum_{\alpha\beta} \sum_{ij} \tilde{\epsilon}_{ii}^{\alpha}(x)\tilde{\epsilon}_{jj}^{\beta}(x) q^0 \left(\frac{\sigma}{3}\right)^2 I_{ij} \right\} \tag{82}$$

with the total partition function given by

$$[Z^n] = \int \mathcal{D}\{q\} \exp\left\{ nN\frac{J^2}{2}q^2 + nN[\ln z_1]_{\vec{y}} + \ln z^{\rm inh}(q) \right\}. \tag{83}$$

Here z_1 is given by Eq. (42) for $M = \bar{\epsilon} = 0$

$$z_1 = \mathop{\rm Tr}_{\{\vec{s}\}} \exp\left\{ J\vec{y}\cdot\vec{s} - \frac{J^2 q}{6}\sum_{ij} s_i I_{ij} s_j \right\}. \tag{84}$$

q^0 has to be evaluated with z_1

$$2q^0 = [\langle\vec{s}\rangle_{z_1}\langle\vec{s}\rangle_{z_1}]_{\vec{y}} \tag{85}$$

and $\vec{y}$ denotes a Gaussian random field with $[y_i y_j] = (q/3)I_{ij}$. The interaction between different replicas in Eq. (82) can be decoupled by introducing a local *random* stress $\sigma_{ii}^{\rm ran}(x)$ with zero mean and variance

$$[\sigma_{ii}^{\rm ran}(x)\sigma_{jj}^{\rm ran}(x')] = q^0\left(\frac{\sigma}{3}\right)^2 I_{ij}\,\delta(x-x'). \tag{86}$$

We can then perform the limit $n \to 0$ and find

$$\lim_{n\to 0}\left(\frac{1}{n}\ln z^{\rm inh}\right) = [\ln \tilde{z}^{\rm inh}]_\sigma \tag{87}$$

with

$$\tilde{z}^{\rm inh} = \int \mathcal{D}\epsilon \exp\left\{ -\tfrac{1}{2}\sum_x \sum_{ijkl} \tilde{\epsilon}_{ij}(x)\tilde{\epsilon}_{kl}(x)\tilde{C}_{ijkl} + \sum_x \sum_i \tilde{\epsilon}_{ii}(x)\sigma_{ii}^{\rm ran}(x) \right\} \tag{88}$$

and partially renormalized elastic constants $\tilde{C}_{ijkl} = C_{ijkl}^0 - (q^0/3)\delta_{ij}\delta_{kl}I_{ik}$. The local static stress gives rise to a local static displacement

$$\langle u_i(\vec{x})\rangle = \int d^3x' G_{ij}(x-x')\frac{\partial}{\partial x_j'}\sigma_{jj}^{\rm ran}(x'), \tag{89}$$

where $G_{ij}(x)$ is the Green's function of the lattice. It can be calculated in Fourier space

$$\tilde{C}_{ijkl}k_j k_l G_{kr} = \delta_{ir}. \tag{90}$$

For an isotropic elastic medium the Green's function in real space is also known,[14] whereas for cubic symmetry the Fourier back transformation is not known in general. Here we just note that $\tilde{\mathbf{C}}$ is given by the bare elastic constant and the *local susceptibility*. Hence the corresponding compliance $\tilde{\mathbf{S}} = \tilde{\mathbf{C}}^{-1} = \mathbf{S}^0 + \mathbf{S}^0\mathbf{K}\chi^{\rm loc}\mathbf{K}^T(\mathbf{S}^0)^T$ always remains finite.

The local static strain vanishes on the average

$$[\langle u_i(\vec{x})\rangle]_\sigma = 0 = [\langle\tilde{\epsilon}_{ij}(\vec{x})\rangle]_\sigma \tag{91}$$

but has a nonzero variance, independent of $\vec{x}$

$$\begin{aligned}[\langle\tilde{\epsilon}_{ii}(\vec{x})\rangle\langle\tilde{\epsilon}_{jj}(\vec{x})\rangle]_\sigma &= \sum_{kl}\int d^3y\int d^3z\, G_{ik}(x-y)G_{jl}(x-z)\left(\frac{\partial}{\partial y_k}\sigma^{\text{ran}}_{kk}(y)\frac{\partial}{\partial z_l}\sigma^{\text{ran}}_{ll}(z)\right)_\sigma \\ &= \sum_{kl}\int d^3y\int d^3z\, G_{ik}(x-y)G_{jl}(x-z)q^0\left(\frac{\sigma}{3}\right)^2 I_{kl}\frac{\partial}{\partial y_k}\frac{\partial}{\partial z_l}\delta(y-z) \\ &= \sum_{kl}q^0\left(\frac{\sigma}{3}\right)^2 I_{kl}\int d^3y\int d^3z\, G_{ik}(y)G_{jl}(z)\frac{\partial}{\partial y_k}\frac{\partial}{\partial z_l}\delta(y-z).\end{aligned} \tag{92}$$

To lowest order in σ or close to T_c: $q^0 \approx q$, so that the spin-glass transition temperature is according to Eq. (62)

$$\left(\frac{T_G}{J}\right)^2 = 1+\left(\frac{\sigma}{3J}\right)^2\left(\frac{\sigma}{3}\right)^2\sum_{ijkl}\int d^3y\int d^3z\, G_{ik}(y)G_{jl}(z)I_{ij}I_{kl}\frac{\partial}{\partial y_k}\frac{\partial}{\partial z_l}\delta(y-z). \tag{93}$$

The most prominent effect of a local strain will be an elastic peak in the van Hove correlation function, as seen experimentally in neutron scattering. The differential cross section for neutrons with energy transfer $\hbar\omega$ and momentum transfer $\hbar\vec{\kappa}$ is proportional to the Fourier transform of the density correlation

$$S(\vec{\kappa},\omega) = \int dt\; e^{i\omega t}\frac{1}{N}\sum_{xy}e^{i\vec{\kappa}\cdot(\vec{l}_x-\vec{l}_y)}\langle e^{i\vec{\kappa}\cdot\vec{u}(\vec{x},0)}e^{-i\vec{\kappa}\cdot\vec{u}(\vec{x},t)}\rangle. \tag{94}$$

Here $\vec{l}_x$ denotes a lattice vector. Local time persistent displacements give rise to an elastic peak $S(\vec{\kappa},\omega) = f(\vec{\kappa})S\omega$ with strength

$$f(\vec{\kappa}) = \frac{1}{N}\sum_{xy}e^{i\vec{\kappa}\cdot(\vec{l}_x-\vec{l}_y)}[\langle e^{i\vec{\kappa}\cdot\vec{u}(\vec{x})}\rangle_{\text{inh}}\langle e^{-i\vec{\kappa}\cdot\vec{u}(\vec{x})}\rangle_{\text{inh}}]_{\sigma^{\text{inh}}}. \tag{95}$$

The thermal average $\langle\cdots\rangle_{\text{inh}}$ has to be calculated with $\tilde{z}^{\text{inh}}$ [Eq. (88)] for *fixed* σ^{ran}. Above the glass transition temperature T_G the elastic component vanishes. Below T_G, its strength $f(\vec{\kappa})$ can be calculated within the approximations of the last section, i.e., a second-order cumulant expansion for $\tilde{\epsilon}\vec{x}$) and long-range interactions for the orientational degrees of freedom. Work along these lines is in progress.

How are these results modified, if the interaction between the orientational degrees of freedom is *short ranged*? The transition to the ferromagnetically ordered state survives for all p in three dimensions. For $p = 3$ and $p = 4$ it is extremely weakly first order with a corresponding enormous increase in the susceptibility, as shown by elaborate Monte Carlo simulations.[25] Hence we expect to find a tetragonal phase for $p = 3$ and a rhombohedral phase for $p = 4$ in a three-dimensional model with short-range interactions. Of course the transition temperatures will be different from the predictions based on mean-field theory. The strong enhancement of ferromagnetic fluctuations as the transition is approached will lead to a corresponding strong decrease of the elastic constants, as is entailed in the exact relation of Eq. (23).

Whether or not there is a glass transition in the three-dimensional short-range model is still a matter of debate. Monte Carlo simulations of the isotropic quadrupolar glass[15] show a static freezing transition at $T = 0$. Carmesin[26] has obtained some evidence that the anisotropy in the quadrupolar glass is essential for a finite $T_G \neq 0$. However the limit of strong anisotropy, i.e., the Potts model in three dimensions, is still controversial. Banavar and Cieplak[27] argued that it depends on the distribution of the randomness whether or not a three-dimensional Potts glass exists at finite temperature. Scheucher *et al.*[28] present evidence that the $p = 3$ Potts model with Gaussian disorder is at its lower critical dimension at $d = 3$.

From a theoretical point of view it is not even clear whether the quadrupolar interaction in three dimensions is in the universality class of the short-range model.

VI. THE SIX-STATE CASE

In this section we discuss the case in which orientations align parallel to one of the face diagonals [Fig. 1(c)]. First the corresponding six-state model with appropriate symmetry will be discussed without consideration of elastic degrees of freedom. Several ordered and glassy states are shown to exist for this model. Then it is argued that (like in the case of the three- and four-state models) weak coupling between elastic and orientational degrees of freedom is not expected to change the phase diagram qualitatively. Equations (17) and (23) can then be used to derive macroscopic distortions and elastic constants in the different phases.

A. Symmetry of the model

All face diagonals are equivalent. Every face diagonal can be mapped on every other by cubic transformations (changing of coordinate axes, reflection of a coordinate axis). Since none of the face diagonals is singled out, the high-temperature phase has vanishing mean orientation.

In order to discuss the interaction of two orientable molecules, the symmetry of *pairs* of orientations has to be considered. It can easily be seen that two pairs of face diagonals can be mapped onto one another by cubic transformations, if and only if they enclose the same angle. Angles can take the values 0, $\pi/3$, or $\pi/2$. In Fig. 1(c) we numbered the face diagonals such that they are perpendicular if $|\mu-\nu| = 3$ and inclose $\pi/3$ if $|\mu-\nu| = 1, 2, 4,$ or 5.

A Hamiltonian of a homogeneous system can be written as

$$H = -\sum_{(x,x')}\sum_{\mu\nu} s_\mu(x) J_0^{\mu\nu} s_\nu(x'). \tag{96}$$

Here, (x, x') are pairs of interacting orientations and the $\vec{s}(x)$ are six-dimensional Potts vectors:

$$\vec{s}(x) = \vec{e}^{\,r(x)}, \quad \text{where } e^r_\mu \equiv I_{r\mu} \equiv 6\delta^{r\mu} - 1. \tag{97}$$

The matrix elements $J_0^{\mu\nu}$ must have the corresponding symmetry, and thus take on three different values: one for $\mu = \nu$, one for $|\mu-\nu| = 3$, and one for all other entries. Matrices of this form will occur frequently, so we define

$$\mathbf{W}(a+b, a-b) \equiv \begin{pmatrix} a & 0 & 0 & b & 0 & 0 \\ 0 & a & 0 & 0 & b & 0 \\ 0 & 0 & a & 0 & 0 & b \\ b & 0 & 0 & a & 0 & 0 \\ 0 & b & 0 & 0 & a & 0 \\ 0 & 0 & b & 0 & 0 & a \end{pmatrix}, \tag{98}$$

where $a+b$ and $a-b$ are the (threefold) eigenvalues of $\mathbf{W}$. If an appropriate zero energy is defined, $J_0^{\mu\nu} = W^{\mu\nu}(J_0^+, J_0^-)$.

Now we introduce quenched disorder without breaking the global symmetry. This leads to several new parameters even if fluctuations of the interaction are Gaussian (see Appendix A). In the model glass discussed below, each realization of the disorder respects the symmetry, i.e., $J^{\mu\nu}_{xx'} = W^{\mu\nu}(J^+_{xx'}, J^-_{xx'})$. The Hamiltonian is

$$H = -\sum_{(x,x')}\sum_{\mu\nu} s_\mu(x)(J_0^{\mu\nu} + \Delta^{x,x'} J^{\mu\nu}) s_\nu(x'), \tag{99}$$

where $J^{\mu\nu} = W^{\mu\nu}(J^+, J^-)$ and $\Delta^{x,x'}$ are uncorrelated, Gaussian random variables with $[\Delta^{x,x'}] = 0$ and $[(\Delta^{x,x'})^2] = 1$. The distribution $p(J^+_{xx'}, J^-_{xx'})$ of our model is shown in Fig. 6. Here the fluctuations $J^+_{xx'}$ and $J^-_{xx'}$ are not independent. We also considered statistically independent distributions $p(J^+_{xx'}, J^-_{xx'}) = \omega(J^+_{xx'}) \cdot \omega(J^-_{xx'})$ with Gaussian ω. The pure glass phase turns out to be exactly the same as for the distribution of Fig. 6, whereas we expect changes in the mixed phases.

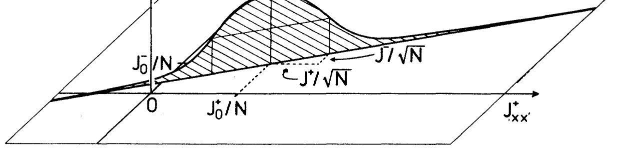

FIG. 6. Probability distribution of the s-s couplings $J^+_{xx'}$ and $J^-_{xx'}$ for model C.

We do not discuss the whole four-dimensional phase diagram but emphasize three important limits: (1) the homogeneous, uniform model; (2) the pure glass with no effective homogeneous interaction; (3) the stability of the thermally disordered, "paramagnetic" phase.

B. The homogeneous six-state model

In mean-field approximation the uniform Hamiltonian reads

$$H = -\frac{1}{N}\sum_{x<x'}\sum_{\mu\nu} s_\mu(x) J_0^{\mu\nu} s_\nu(x'). \tag{100}$$

It is required that parallel alignments have lowest energy, i.e., $J_0^- > 0$ and $J_0^+ > -J_0^-$. Otherwise the model is fully frustrated in mean-field approximation and one expects a high degeneracy of the ground state.

We are interested in the expectation value of the mean orientation:

$$\vec{m}\left(\frac{J_0^+}{T}, \frac{J_0^-}{T}\right) = \frac{1}{N}\sum_x \langle \vec{s}(x)\rangle. \tag{101}$$

Then

$$n_\mu \equiv \tfrac{1}{6}(m_\mu + 1) \tag{102}$$

is the average fraction of defects, which are oriented parallel to axis μ.

It can be found by large deviation theory that $\vec{m}$ minimizes the function

$$f(\vec{m}) = -\frac{1}{2}\vec{m}^T \mathbf{J}_0 \vec{m} + \frac{T}{6}\sum_\mu (m_\mu + 1)\ln(m_\mu + 1) \tag{103}$$

under the constraint $\sum_\mu m_\mu = 0$. Figure 7 shows the phase diagram. At high temperatures the orientations

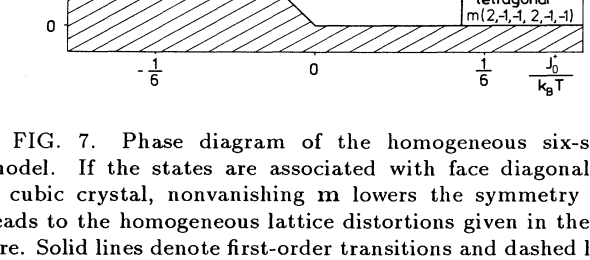

FIG. 7. Phase diagram of the homogeneous six-state model. If the states are associated with face diagonals in a cubic crystal, nonvanishing $\mathbf{m}$ lowers the symmetry and leads to the homogeneous lattice distortions given in the figure. Solid lines denote first-order transitions and dashed lines denote second-order transitions.

are thermally disordered: $\vec{m} = 0$. The ground state is characterized by parallel orientations of all defects, i.e., $\vec{n} = (1,0,0,0,0,0)$ and $\vec{m} = (5,-1,-1,-1,-1,-1)$. The ground state is sixfold degenerate (orientations 2–6 are of course equally likely). When the temperature is slightly above zero, almost all defects will be parallel to the (say) 1-direction. The local field, "felt" by the defect at x is $\vec{h} = \mathbf{W}(J_0^+, J_0^-)\vec{m} + O(1/N)$. Now assume that $m_2 = m_4$. Multiplication by $\mathbf{W}(J_0^+, J_0^-)$ will in general lead to $h_2 \neq h_4$, which is inconsistent with the assumption. So one should expect that at low temperatures the mean orientation has the symmetry

$$\vec{m} = (m_1, m, m, m_4, m, m), \tag{104}$$

where $m = -(m_1 + m_4)/4$ is imposed by $\sum_\mu m_\mu = 0$. This is exactly what is found by explicit calculation.

If $J_0^+ \gg J_0^-$, the system enters an intermediate phase on cooling from high temperatures. Here the mean orientation is

$$\vec{m} = m(2,-1,-1,2,-1,-1). \tag{105}$$

The state is threefold degenerate. Obviously it has lower symmetry than the disordered phase, as one pair of orthogonal orientations is selected by spontaneous symmetry breaking. However, it has higher symmetry than the low-temperature phase, because there is no distinction within the pair ($m_1 = m_4$).

For $-J_0^- \approx J_0^+ < 0$ another intermediate phase is observed. Here we find no distinction between pairs (1,4), (2,5), and (3,6) but one orientation in every pair is preferred. There are 2^3 ways to choose the preferred orientations, hence the degeneracy is eightfold. $\vec{m}$ is, e.g.,

$$\vec{m} = m(1,1,1,-1,-1,-1). \tag{106}$$

Note that the three preferred orientations ($m_\mu = +m$) lie in a plane if $m_1 \cdot m_2 \cdot m_3 = -m^3$ [Fig. 8(a)] and align around a body diagonal if $m_1 \cdot m_2 \cdot m_3 = +m^3$ [Fig. 8(b)]. However the system does not discriminate between the two possibilities (which are important in view of corresponding lattice distortions). This is due to the fact that the Hamiltonian involves only pair interactions and every two out of the three preferred orientations have an angle $\pi/3$ in both cases, but one must look at three orientations at a time to distinguish between the two cases.

In the cubic high-temperature phase (see Fig. 7) the system has highest symmetry. The symmetry is lowest in the orthorhombic phase because $\vec{m}$ [Eq. (104)] contains two independent order parameters m_1, m_4. Note however that there is still some symmetry left: $m_2 = m_3 = m_5 = m_6$. The same relations hold in the tetragonal phase, where we have in addition $m_1 = m_4$. The orthorhombic phase represents thus a subsymmetry of the tetragonal phase. The phase transition is second order and $\vec{m}(T)$ is continuous for $T < 6J^+$. On the other hand the orthorhombic phase is not a subsymmetry of the rhombohedral phase (106), because in the latter case $m_2 \neq m_5$. Hence the order parameter $\vec{m}$ jumps and the phase transition is first order. The cubic-tetragonal transition corresponds to the paramagnetic → ferromagnetic transition of the $p = 3$ Potts magnet (see Sec. VII). For $J^+ = J^-$ the system is an isotropic Potts magnet (cubic-orthorhombic transition) with $p = 6$. Both transitions are first order in mean-field approximation, although this is not required by a simple symmetry argument.

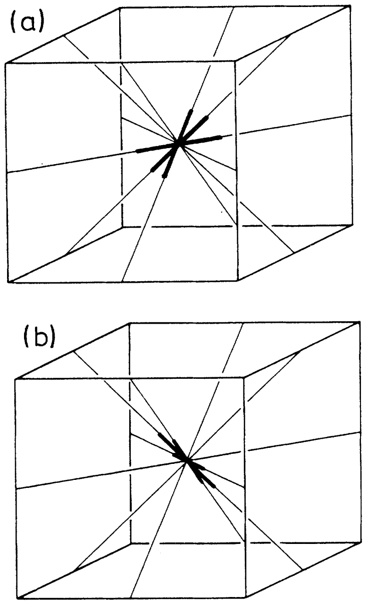

FIG. 8. In the rhombohedral phase three face diagonals enclosing angles $\pi/3$ are favored. They align around one of the body diagonals (a) or lie in a plane perpendicular to a body diagonal (b).

C. The six-state glass

Starting from (99) we replicate the partition function and take the average over $\Delta^{xx'}$. Additive constants are dropped to obtain

$$[Z^n] = \operatorname*{Tr}_{\{\vec{s}^{\,\alpha}(x)\}} \exp\Bigg\{ \frac{\beta}{2N} \sum_\alpha \sum_{\mu\nu} \Big(\sum_x s_\mu^\alpha(x)\Big) \hat{J}_0^{\mu\nu} \Big(\sum_x s_\nu^\alpha(x)\Big) + \frac{\beta^2}{2N} \sum_{\alpha<\beta} \sum_{\mu\nu\rho\sigma} \Big(\sum_x s_\mu^\alpha(x) s_\rho^\beta(x)\Big) J^{\mu\nu} J^{\rho\sigma} \Big(\sum_x s_\nu^\alpha(x) s_\sigma^\beta(x)\Big)\Bigg\}. \tag{107}$$

Here $\hat{\mathbf{J}}_0 \equiv \mathbf{W}(\hat{J}_0^+, \hat{J}_0^-)$ and

$$\hat{J}_0^+ \equiv J_0^+ + \beta(6J^+)^2, \quad \hat{J}_0^- \equiv J_0^- + \beta(6J^-)^2, \tag{108}$$

are the effective homogeneous coupling constants. Gauss transformation yields the free energy per site:

$$\beta f = \min_{\{m,q\}} \Bigg[\frac{\beta}{2} \sum_{\alpha} \sum_{\mu\nu} m_\mu^\alpha (\hat{\mathbf{J}}_0^{-1})^{\mu\nu} m_\nu^\alpha + \frac{\beta^2}{2} \sum_{\alpha<\beta} \sum_{\mu\nu\rho\sigma} q_{\mu\rho}^{\alpha\beta} (\mathbf{J}^{-1})^{\mu\nu} (\mathbf{J}^{-1})^{\rho\sigma} q_{\nu\sigma}^{\alpha\beta} - \ln \operatorname*{Tr}_{\{\vec{s}^\alpha\}} \exp\Bigg(\beta \sum_{\alpha} \sum_{\mu} m_\mu^\alpha s_\mu^\alpha + \beta^2 \sum_{\alpha<\beta} \sum_{\mu\rho} q_{\mu\rho}^{\alpha\beta} s_\mu^\alpha s_\rho^\beta \Bigg) \Bigg]. \tag{109}$$

Note that the special structure of the system, represented by $\hat{\mathbf{J}}_0$ and $\mathbf{J}$, appears only in terms quadratic in $\vec{m}$ and $\mathbf{q}$. We need not specify the interactions yet. If, e.g., $\hat{\mathbf{J}}_0$ and $\mathbf{J}$ were proportional to the identity matrix, Eq. (109) would describe the isotropic (p=6) Potts glass.[19,24]

The extremal values of $\vec{m}$ and $\mathbf{q}$ ($\vec{m}^0$ and $\mathbf{q}^0$) correspond to the magnetization and Edwards-Anderson order parameter:

$$\frac{1}{N} \sum_x [\langle \vec{s}^\alpha(x) \rangle] = \hat{\mathbf{J}}_0^{-1} \cdot \vec{m}^0, \quad \frac{1}{N} \sum_x [\langle \vec{s}^\alpha(x) (\vec{s}^\beta(x))^T \rangle] = \mathbf{J}^{-1} \mathbf{q}^0 \mathbf{J}^{-1}. \tag{110}$$

In order to obtain the stability boundary of the high-temperature phase ($m_\mu^\alpha = 0, q_{\mu\nu}^{\alpha\beta} = 0$) the trace in Eq. (109) has to be expanded up to second order in m and q

$$\operatorname*{Tr}_{\{\vec{s}^\alpha\}} \exp\Bigg\{ \beta \sum_{\alpha} \sum_{\mu} m_\mu^\alpha s_\mu^\alpha + \beta^2 \sum_{\alpha<\beta} \sum_{\mu\rho} q_{\mu\rho}^{\alpha\beta} s_\mu^\alpha s_\rho^\beta \Bigg\} = 6^n \Bigg(1 + \frac{\beta^2}{2} \sum_{\alpha} \sum_{\mu\nu} m_\mu^\alpha I^{\mu\nu} m_\nu^\alpha + \frac{\beta^4}{2} \sum_{\alpha<\beta} \sum_{\mu\nu\rho\sigma} q_{\mu\nu}^{\alpha\beta} I^{\mu\rho} I^{\nu\sigma} q_{\rho\sigma}^{\alpha\beta} + O(m^3, m^2 q, m q^2, q^3) \Bigg). \tag{111}$$

The high-temperature phase is (at least) metastable, if the m-m and q-q coupling matrices are positive definite, which means that

$$\frac{T}{6} > \hat{J}_0^+, \hat{J}_0^-, J^+, J^-. \tag{112}$$

Figure (9) shows two two-dimensional cuts of the four-dimensional phase diagram. Note the similarity to the Potts glass (Fig. 2).

The result can be generalized for all p-state models with coupling matrices which do not single out one or more states. To be more precise, we require that $(1, 1, \ldots, 1)$ be an eigenvector of $\mathbf{J}_0$ and $\mathbf{J}$.Then the high-temperature phase is (meta-)stable for T/p greater than all Eigenvalues of $\mathbf{J}_0$ and $\mathbf{J}$.

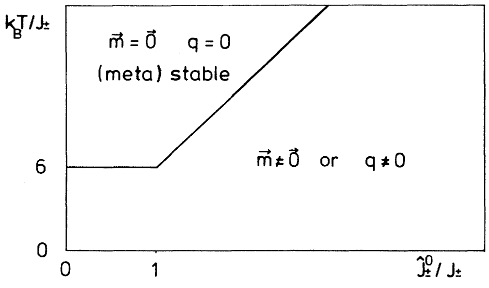

FIG. 9. The "paramagnetic" solution $\mathbf{m} = \mathbf{0}$ of the six-state glass is at least metastable if $T/6 > \hat{J}_0^+, \hat{J}_0^-, J^+, J^-$. We show here two two-dimensional cuts of the phase diagram to stress the similarity to the Potts glass (Fig. 2).

D. Pure glass phase

In the following we put $\hat{J}_0^\pm = 0$ and consider only replica symmetric solutions. In the absence of an effective homogeneous coupling no global preference of an orientation is expected, i.e.,

$$\frac{1}{N} \sum_x [\langle \vec{s}(x) \rangle] = \vec{0} \rightarrow \vec{m} = \vec{0}. \tag{113}$$

(We write $\vec{m}, \mathbf{q}$ instead of $\vec{m}^0, \mathbf{q}^0$ in the following.) However, for a specific realization of $\Delta^{xx'}$ the defect at site x may be frozen:

$$\langle \vec{s}(x) \rangle \neq 0. \tag{114}$$

This leads to a nonvanishing Edwards-Anderson order parameter

$$\frac{1}{N} \sum_x [\langle s_\mu(x) \rangle \langle s_\nu(x) \rangle] \neq 0 \rightarrow q_{\mu\nu} \neq 0. \tag{115}$$

In addition to (113) we require that for $\hat{J}_0^\pm = 0$, $q_{\mu\nu}$ should have the symmetry of the Hamiltonian, i.e., of $W^{\mu\nu}$. Then

$$q_{\mu\nu} = W^{\mu\nu}(q^+, q^-) - \frac{q^+}{6}. \tag{116}$$

Here we already took care of the condition

$$\sum_{\mu} q_{\mu\nu} = 0, \tag{117}$$

which originates from our Potts spin representation of the states:

$$\sum_{\mu} s_\mu(x) = \sum_{\mu} e_\mu^{r(x)} = \sum_{\mu} (6\delta^{\mu,r(x)} - 1) = 0. \tag{118}$$

The eigenvalues of the matrix $q_{\mu\nu}$ are (1×) 0, (2×) q^+, and (3×) q^-. So the system is described by two order parameters q^+ and q^-. Before we turn over to the results of the calculation, let us discuss the physical meaning of q^+ and q^-. We define the vectors $\vec{v}^k$ by

$$\{\vec{v}^1, \ldots, \vec{v}^8\} = \left\{ \pm \begin{pmatrix} -1 \\ 1 \\ 1 \\ 1 \\ -1 \\ -1 \end{pmatrix}, \pm \begin{pmatrix} 1 \\ -1 \\ 1 \\ -1 \\ 1 \\ -1 \end{pmatrix}, \pm \begin{pmatrix} 1 \\ 1 \\ -1 \\ -1 \\ -1 \\ 1 \end{pmatrix}, \pm \begin{pmatrix} 1 \\ 1 \\ 1 \\ -1 \\ -1 \\ -1 \end{pmatrix} \right\}. \tag{119}$$

Remember that in the homogeneous system there is a phase (rhombohedral), where $\vec{m}$ and $(1/N)\sum_x [\langle \vec{s}(x) \rangle]$ are parallel to one of these directions. Now assume that in the glass phase the local mean orientation at site x, $\langle \vec{s}(x) \rangle$ is parallel to $\vec{v}^{k(x)}$. If each k is equally probable, then $(1/N)\sum_x [\langle \vec{s}(x) \rangle] = \vec{0}$, i.e., the global mean orientation vanishes as we claimed for the pure glass phase. The order parameter of this phase has the following structure:

$$\frac{1}{N} \sum_{x} [\langle s_\mu(x) \rangle \langle s_\nu(x) \rangle] \sim \frac{1}{8} \sum_{k=1}^{8} v_\mu^k v_\nu^k \sim W^{\mu\nu}(0,1), \tag{120}$$

which implies that $q^+ = 0$. Now assume that local orientations freeze into states which prefer one pair of orthogonal face diagonals. Here $\langle \vec{s}(x) \rangle$ is parallel to

$$\{\vec{v}^1, \vec{v}^2, \vec{v}^3\} = \left\{ \begin{pmatrix} 2 \\ -1 \\ -1 \\ 2 \\ -1 \\ -1 \end{pmatrix}, \begin{pmatrix} -1 \\ 2 \\ -1 \\ -1 \\ 2 \\ -1 \end{pmatrix}, \begin{pmatrix} -1 \\ -1 \\ 2 \\ -1 \\ -1 \\ 2 \end{pmatrix} \right\} \tag{121}$$

and $q^- = 0$.

So we should associate $q^+ \neq 0$ with local freezing of orthogonal pairs and locally tetragonal structure and $q^- \neq 0$ with local splitting of occupation numbers within pairs and locally rhombohedral structure. A freezing of $\langle \vec{s}(x) \rangle$ parallel to (m_1, m, m, m_4, m, m) directions causes both $q^+ \neq 0$ and $q^- \neq 0$ as the six states break both symmetries.

The phase diagram (Fig. 10) is constructed from an expansion of the free energy:

$$\begin{aligned} \frac{f}{n} = {} & 2\left[\left(\frac{T}{6J+}\right)^2 - 1\right] 3^2(q^+)^2 + 3\left[\left(\frac{T}{6J^-}\right)^2 - 1\right] 3^2(q^-)^2 + 2^2 3^3 (q^+)^3 - 2^2 3^4 q^+(q^-)^2 + 2^3 3^3 (q^-)^3 \\ & -2 \cdot 3^5 (q^+)^4 + 2^2 3^6 (q^+)^2 (q^-)^2 + 2^5 3^5 q^+ (q^-)^3 - 2^2 3^6 (q^-)^4 + O(q^5). \end{aligned} \tag{122}$$

The thermally disordered phase, $q^+ = q^- = 0$ locally minimizes the free energy for $J^+, J^- < T/6$. For $J^+ > J^-$ we find a second-order transition to $q^+ \neq 0$ but $q^- = 0$. (Note that f does not contain a term linear in q^-.) q^+ grows linearly in $T - T_c$ [Fig. 11(a)]. In this region we expect a glassy phase with a local tetragonal structure. For $J^- > J^+$ the system undergoes another second-order transition to a phase with $q^+ \neq 0$ and $q^- \neq 0$. [Note the terms $q^+(q^-)^2$ and $q^+(q^-)^3$ in f.] Here q^- grows linearly in $T - T_c$ whereas $q^+ \sim (T - T_c)^2$ [Fig. 11(b)]. So just above the transition line ($T = 6J^-$): $q^+ \ll q^-$ and we expect a glassy phase with almost pure local rhombohedral structure.

The expansion (124) of the free energy is not stable as $(q^+)^4$ and $(q^-)^4$ have negative coefficients. To recover stability one has to take into account higher powers of q, at least up to q^6. In particular in the shaded area we do not even get a metastable solution. However, it is quite obvious that it should have $q^+ \neq 0$ and $q^- \neq 0$. For $J^+ = J^-$ the system is the six-state Potts glass.[19,24] The phase boundary between $q^- = 0$ and $q^- \neq 0$ has slope $-\frac{4}{3}$ in the neighborhood of the tricritical point $J^+ = J^- = T/6$. The borderline of the shaded area has slope $-\frac{2}{3}$ in this region. Both lines have been derived for $q^+, q^- \ll 1$.

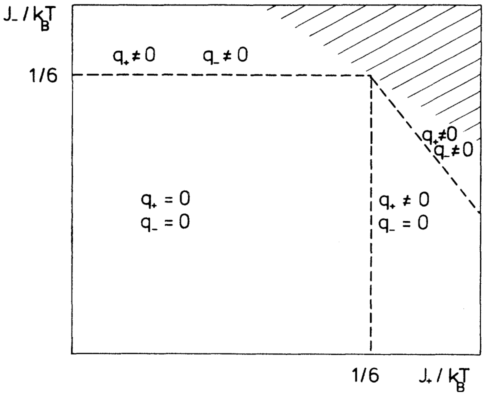

FIG. 10. Phase diagram of the pure six-state glass. The free energy has been expanded up to fourth order in q. In the shaded area we find no stable solution. All transitions are second order.

E. Elastic properties

As we have shown, the model defined by (99) exhibits several phases: (1) a thermally disordered high-temperature phase; (2) ordered phases with nonzero global orientation with different symmetries for $\mathbf{J} \ll \hat{\mathbf{J}}_0$; (3) pure glass phases with frozen local orientations for $\mathbf{J} \gg \hat{\mathbf{J}}_0$.

In addition there may be mixed phases for an intermediate range of parameters and low temperatures.

Orientations are coupled to elastic degrees of freedom by adding

$$\sum_x \sum_\mu s_\mu(x)\tilde{\sigma}^\mu \cdot \epsilon(x) \tag{123}$$

to the Hamiltonian.

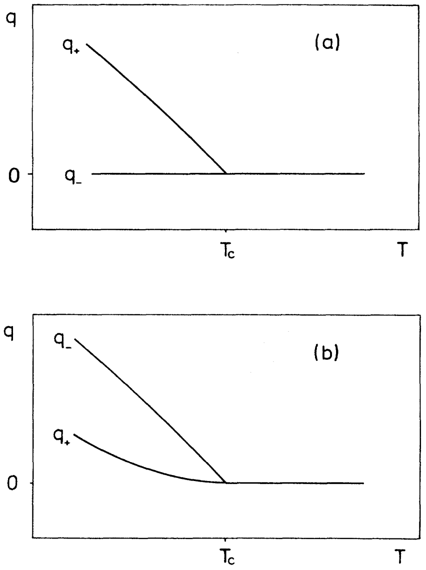

FIG. 11. For the pure glass with $J^+ > J^-$ (a) one enters an intermediate phase on cooling with $q^- = 0, q^+ \neq 0$. At the transition q^+ grows linearly in $T_c - T$. For $J^+ < J^-$ (b) q^- grows linearly whereas q^+ is quadratic in $T_c - T$.

$\tilde{\sigma}^\mu$ is given by (7) and its cubic transformations. We put $\sigma_0 = 0$ by a readjustment of the lattice constant.

The full Hamiltonian is given by Eq. (11). Expectation values of orientations and elastic distortions are related by Eq. (17). We showed for the three- and four-state models that weak ϵ-s coupling, $\beta\sigma_{L,T} \ll 1$, does not alter the phase diagram qualitatively. In particular the symmetry of orientational expectation values remains unchanged. Here it is assumed that this result can be generalized to the six-state case. Then the orientational expectation values on the right-hand side of Eqs. (17) and (23) can be taken from the discussion of the Hamiltonian (99). They lead to elastic distortions with different symmetries (Fig. 7): (1) high-temperature phase → cubic; (2) $\vec{m} = m(2,-1,-1,2,-1,-1)$ → tetragonal; (3) $\vec{m} = m(1,1,1,-1,-1,-1)$ → rhombohedral; (4) $\vec{m} = (m_1, m, m, m_4, m, m)$ → orthorhombic; (5) pure glass → cubic with frozen local strain.

It is also straightforward to show that a mean orientation $\vec{m} = (m_1, m_1, m, m_4, m_4, m)$ would cause a monoclinic distortion. This phase is unstable in the homogeneous limit ($J^\pm = 0$).

It has already been mentioned above that two rhombohedral phases are accessible for the system, depending on the sign of $m_1 m_2 m_3 = \pm m^3$. For $\sigma_T < 0$ and $m_1 m_2 m_3 = +m^3$ the crystal is stretched along a body diagonal, whereas in the $m_1 m_2 m_3 = -m^3$ case it will be shortened along the body diagonal and stretched in the perpendicular plane. If $\sigma_T > 0$, the two cases will be interchanged. In our simple model both configurations are degenerate. However, higher-order terms or short-range contributions presumably distinguish between the two possibilities.

In the pure glass phase, $\vec{m} = \vec{0}$ and there is no macroscopic distortion. Nevertheless the elastic constants are affected by the disordered freezing of orientations. The elastic compliance can be calculated as in Sec. V:

$$\begin{aligned}
S_{1111} - S^0_{1111} &= 2\left(1 - \frac{q^+}{6(J+)^2}\right)(S^0_{1111} - S^0_{1122})^2\sigma_L^2, \\
S_{1122} - S^0_{1122} &= -\left(1 - \frac{q^+}{6(J+)^2}\right)(S^0_{1111} - S^0_{1122})^2\sigma_L^2, \\
S_{1212} - S^0_{1212} &= \frac{1}{9}\left(1 - \frac{q^-}{(J^-)^2}\right)(S^0_{1212})^2\sigma_T^2.
\end{aligned} \tag{124}$$

VII. DIPOLAR EFFECTS

The symmetry arguments, which have been used to derive the Hamiltonians of our three-, four-, and six-state models, can easily be generalized to treat arbitrary p-state models. In particular we are now ready to discuss systems with dipolar defects for which the Hamiltonian is not invariant under 180 degree flips of a defect.

As an example we return to the three-state model, where the orientable molecules align along coordinate axes. Now the two ends of the defect axis are no longer equivalent. Each molecule is in one of six states (Fig. 12), modeled by Potts vectors: $\vec{s}(x)$ (97). Cubic symmetry is assumed and the $\vec{s}$-$\vec{s}$ interaction matrices $\mathbf{J}$ take the form (98).

Hence we exactly recover the six-state model, which applies to nondipolar face-diagonal symmetry, with however a different physical interpretation of the states and phases. If dipolar effects vanish, the system cannot distinguish between state 1 and state 4, i.e., $J^- = 0$. So J^- is a measure of the dipolar interaction strength. Analogously J^+ measures the quadrupolar (nondipolar) interaction.

The phases can be described by $\vec{m}$ and $\mathbf{q}$. If the nonordered pairs $\{m_1, m_4\}$, $\{m_2, m_5\}$, $\{m_3, m_6\}$ are all equal (e.g., $\{m, -m\}$, $\{m, -m\}$, $\{-m, m\}$) the phase will be called quadrupolarly disordered (qu.d). Otherwise the phase is quadrupolarly ordered (qu.o), which means that (at least) one of the coordinate axes is discriminated. If $m_1 = m_4$, $m_2 = m_5$, and $m_3 = m_6$, the phase will be called dipolarly disordered (di.d), otherwise di.o.

The form of the orientation-strain coupling σ^μ must be newly determined. Let us assume that the defect points in the $+x$ direction correspond to $\mu = 1$. Then the force dipole tensor σ_{ij} must be invariant under rotations around the $\hat{x}$ axis by $\pi/2$ and π. Hence σ^μ is given by Eq. (7) with $\sigma_T = 0$. This means that only qu.o. phases show a macroscopic distortion, which is always tetragonal. Defects with dipolar symmetry and no quadrupolar moment only couple to nonuniform strains, as already noted in Ref. 29.

For homogeneous couplings (no quenched disorder) we get the phase diagram of Fig. 13. Now assume that J_0^+ and J_0^- are given and T is varied. At high temperatures the crystal is always completely disordered and at low temperatures it has qu.o and di.o. At intermediate temperatures we have three different cases (Fig. 13).

(i) $J_0^+/J_0^- \gg 1$: The system goes into an intermediate phase, which has qu.o but no di.o and hence is tetragonal.

(ii) $J_0^+/J_0^- \approx 1$: The intermediate phase has no qu.o but di.o.

(iii) Quadrupoles and dipoles order simultaneously.

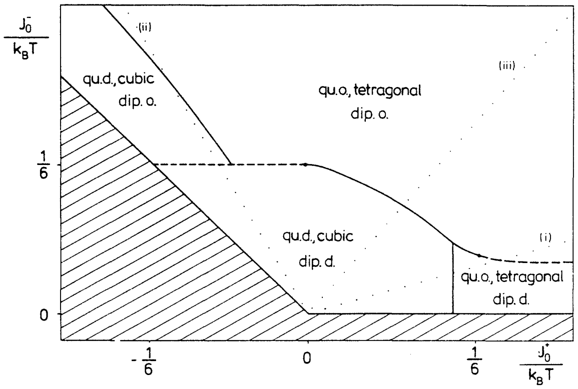

FIG. 13. Phase diagram of the homogeneous, dipolar model A. The system is mathematically identical to the quadrupolar model C as long as the coupling between orientations and lattice distortions is disregarded. Three possible paths which the system can take are indicated as dotted lines (i), (ii), and (iii). The transitions occurring along these paths between quadrupolarly (qu.) and dipolarly (di.) ordered (o.) and disordered (d.) phases are discussed in the main text.

In the pure glass phase, $\hat{\mathbf{J}}_0 = \mathbf{0}$, the elastic constants are not modified by q^-, because $\sigma_T = 0$. Remember that near the glass transition $q^+ \sim (T_c - T)^{\beta_+}$ where β_+ is 1 or 2, depending on the ratio J_0^+/J_0^- (Fig. 11).

If cubic potassium tantalate, KTaO$_3$, is doped with Li or Na, the smaller dopand (say Li) replaces the larger K atom. The former is thus situated in a cage of 12 oxygen atoms, which is too large, so that it takes an off-center position on one of the cubic axes[1] (Fig. 14). We take this position as the orientational degree of freedom. Choosing the center of the cage as the origin, the six possible positions are indicated by the end points of the vectors in Fig. 12. So our model has the appropriate symmetry for the above example. We expect the dipolar interaction to be of electric origin and the dominant quadrupolar inter-

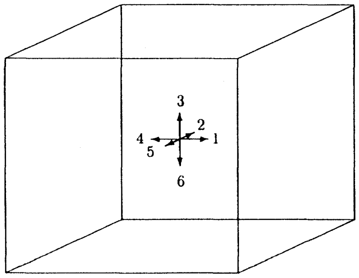

FIG. 12. If the defects have an electric moment, up and down directions have to be distinguished. For the anisotropy of model A we get six states, which can be numbered such that states μ and ν are antiparallel for $|\mu - \nu| = 3$ and perpendicular for $|\mu - \nu| = 1, 2, 4$, or 5.

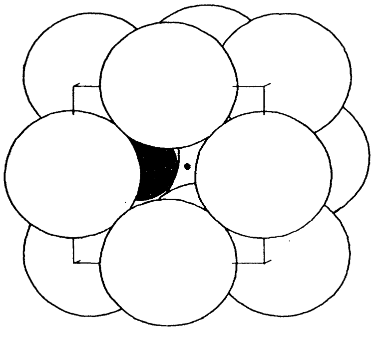

FIG. 14. The dopand Li$^+$ (black) in lithium-potassium tantalate in its cage of the 12 surrounding oxygen atoms (white) takes an off-center position. It can be represented by a vector pointing from the center of the cage (black point) to the center of the Li$^+$-ion. The six possible positions correspond to the vectors in Fig. 12.

action to be mediated by lattice strains, so that dipolar and quadrupolar effects should be separable in dielectric and structural/elastic measurements.

As it has been stated in the beginning of this section, every model with p easy axes can be extended by introducing dipolar interactions. One must exploit the symmetries of the corresponding $2p$ states to reduce the number of free parameters of the $2p \times 2p$ matrix $\mathbf{J}_0$ and the couplings $\tilde{\sigma}^{\mu}$. Even if the ϵ-s coupling $\tilde{\sigma}^{\mu}$ is disregarded, this will become more and more complex for $p > 3$. Consider, for example, the face-diagonal model with dipolar interactions (Fig. 15). It includes four free parameters. The energy can take five different values, depending on whether the angle between orientations is $0, \pi/3, \pi/2, 2\pi/3$, or π; the zero energy is arbitrary. With the numbering of the states of Fig. 15

$$\mathbf{J}_0 = \begin{pmatrix} \mathbf{J}_{\mathrm{I}} & \mathbf{J}_{\mathrm{II}} \\ \mathbf{J}_{\mathrm{II}} & \mathbf{J}_{\mathrm{I}} \end{pmatrix} \tag{125}$$

with

$$\mathbf{J}_{\mathrm{I}} = \begin{pmatrix} a & d & d & c & d & 0 \\ d & a & d & 0 & c & d \\ d & d & a & d & 0 & c \\ c & 0 & d & a & 0 & 0 \\ d & c & 0 & 0 & a & 0 \\ 0 & d & c & 0 & 0 & a \end{pmatrix}, \tag{126}$$

$$\mathbf{J}_{\mathrm{II}} = \begin{pmatrix} b & 0 & 0 & c & 0 & d \\ 0 & b & 0 & d & c & 0 \\ 0 & 0 & b & 0 & d & c \\ c & d & 0 & b & d & d \\ 0 & c & d & d & b & d \\ d & 0 & c & d & d & b \end{pmatrix}.$$

If no dipolar interaction is present, states r and $r+6$ become identical and $a = b$, $d = 0$. It might be convenient to simplify the general interaction [Eqs. (125) and (126)] assuming that the dipolar part has a specific form, controlled by one parameter (instead of two: $a - b, d$). Take, e.g., the scalar product of the vectors in Fig. 15 as the dipolar interaction energy. Then $\mathbf{J}_0$ is a sum of the quadrupolar part (with twice as many states) and the dipolar part:

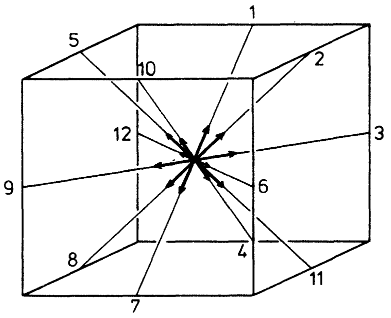

FIG. 15. If dipolar interactions are taken into account for model C, 12 orientations are allowed. Note the numbering of the states: Orientations μ and ν are antiparallel for $|\mu - \nu| = 7$ and perpendicular for $|\mu - \nu| = 3$ or $|\mu - \nu| = 9$.

$$\mathbf{J}_0 = \begin{pmatrix} \mathbf{J}_q & \mathbf{J}_q \\ \mathbf{J}_q & \mathbf{J}_q \end{pmatrix} + d \begin{pmatrix} \mathbf{J}_{d\mathrm{I}} & \mathbf{J}_{d\mathrm{II}} \\ \mathbf{J}_{d\mathrm{II}} & \mathbf{J}_{d\mathrm{I}} \end{pmatrix}, \tag{127}$$

where $\mathbf{J}_q = \mathbf{W}(J^+, J^-)$ is the quadrupolar interaction matrix (98) and

$$\mathbf{J}_{d\mathrm{I}} = \begin{pmatrix} 2 & 1 & 1 & 0 & 1 & -1 \\ 1 & 2 & 1 & -1 & 0 & 1 \\ 1 & 1 & 2 & 1 & -1 & 0 \\ 0 & -1 & 1 & 2 & -1 & -1 \\ 1 & 0 & -1 & -1 & 2 & -1 \\ -1 & 1 & 0 & -1 & -1 & 2 \end{pmatrix},$$

$$\mathbf{J}_{d\mathrm{II}} = -\mathbf{J}_{d\mathrm{I}}. \tag{128}$$

We shall not discuss the details of the three-dimensional phase diagram of this homogeneous model. Let us just mention as a final point that the phases and phase boundaries of the quadrupolar model ($d = 0$) remain unchanged for d/T small enough. The effect can be seen in Fig. 13. Here the quadrupolar model is a three-state Potts system and d corresponds to J^-. For $J^-/T \ll 1$ the system has indeed the same order parameters as for $J^-/T = 0$. The phase boundary does not depend on J^- and the low-temperature phase has qu.o but no di.o.

VIII. CONCLUSIONS

We have proposed several mesoscopic models for the orientational glasses. Basic ingredients for our models are the following.

(1) The orientational degrees of freedom are characterized by a discrete state variable. The number of states is determined by the local anisotropy of the particular substance under consideration and the symmetry of the interaction is specified by the crystal structure. For example, $(\mathrm{KBr})_x(\mathrm{KCN})_{1-x}$ is described by a four-state Potts model, which seems adequate in the vicinity of the critical concentration, $x_c \sim 0.4$, for the glass transition.[22] As another example we refer to $\mathrm{K}_x\mathrm{TaO}_3(\mathrm{Li})_{1-x}$, which may be considered a possible realization of our dipolar six-state model[30,31] which is discussed in Sec. VII.

(2) On mesoscopic length scales the medium is considered as elastic, except for the coupling to the orientational degrees of freedom. This is justified if fluctuations on smaller length scales give rise to a finite renormalization of the elastic constants and do not lead to structural instabilities.

(3) The important interactions are those between the orientational degrees of freedom, which are either mediated by lattice distortions on a small wavelength or of electrostatic origin. These couplings can give rise to cooperative freezing into either random directions or homogeneously ordered states. Hence the cooperative behavior of the orientational degrees of freedom is considered to be the basic mechanism for the observed phase transitions. Modifications of the elastic properties and the crystal structure are due to the bilinear coupling between elastic distortions and orientations. There are of course other mechanisms, which lead to structural phase transitions

accompanied by freezing of orientable molecules. A possible example is pure KCN, where experiments yield evidence for a martensitic transition into an orthorhombic phase.[32,23] Experiments in the high-temperature phase reveal a local anisotropy which is compatible with a four-state model.[33,34] On the basis of our four-state model one would then expect a rhombohedral low-temperature phase, as found in pure CsCN.[35,36]

The models have been solved, using a mean-field approximation for the interaction between the orientational degrees of freedom and a second-order cumulant expansion for the inhomogeneous elastic strain. The main results are the following.

(1) A phase transition to a low-temperature phase with long-range orientational order is observed, provided the homogeneous interaction is strong enough. This transition is always accompanied by homogeneous lattice deformations, which give rise to new crystal structures in the low-temperature phase. For the three-state model, the symmetry of the low-temperature phase is tetragonal, for the four-state model it is rhombohedral, and for the six-state model it can be tetragonal, orthorhombic, or rhombohedral, depending on the anisotropy of the coupling (see Fig. 7). $(\mathrm{KBr})_x(\mathrm{KCN})_{1-x}$ for $x \sim x_c$ may be considered an experimental realization for the four-state model.[22] Li atoms in $\mathrm{K}_x\mathrm{TaO}_3(\mathrm{Li})_{1-x}$ are defects with dipolar and quadrupolar moments. They can be modeled by six state variables (see Fig. 12). As shown in Sec. VII our model allows for independent ordering of the dipolar and quadrupolar moments. Hence there are three possible phases with long-range order: Simultaneous dipolar and quadrupolar ordering, dipolar without quadrupolar ordering, and quadrupolar without dipolar ordering. The experimental situation is not completely clear, but there is evidence for independent freezing of dipolar and quadrupolar moments.[31] As far as the uniform distortion is concerned, the dipolar six-state model is equivalent to the three-state model with a tetragonal low-temperature phase in agreement with experiment.[37,38]

(2) If the interaction between the orientations is sufficiently random, our model predicts freezing of the orientations in random directions, much like the spin-glass phase in magnetic materials. This scenario is supported by a number of experimental results, in particular for the dipolar glasses, where the orientational degrees of freedom can be probed experimentally by dielectric measurements. One finds a cusp in the ac dielectric function and a plateau in the dc dielectric function in analogy to the corresponding susceptibilities in spin glasses.[1] Furthermore one observes irreversible behavior upon cooling. The remanent polarization was found to depend on the history of the sample. Of particular interest are field cooled and zero field cooled measurements.[39,40] Attempts have been made to measure the order parameter susceptibility as the nonlinear dielectric response.[41]

The six-state model allows for a variety of glassy phases. Each glassy phase is characterized by the symmetry of one of the homogeneous low-temperature phases. For example, one finds a glassy phase with local tetragonal distortions, which average to zero, so that the global symmetry of the medium remains cubic. The random freezing of the orientations gives rise to random static strains. These static strain fluctuations show up as a quasielastic peak in the glassy phase. Its intensity is proportional to the glass order parameter.[42] Its wave-vector dependence offers the possibility to detect local order in the glassy phase and possibly discriminate between various glassy phases.

The variety of glassy phases is even larger, if one takes into account the possibility of mixed phases, where homogeneous deformations coexist with glasslike order.

(3) The elastic properties of the medium are affected by cooperative freezing of the orientations, no matter whether this leads to a homogeneously ordered state or a glassy phase. Due to the bilinear coupling of translational and orientational degrees of freedom in our model, there is an exact relation between the elastic constants and the orientational susceptibility. If the system approaches the transition to a homogeneously ordered state, the susceptibility follows a Curie-Weiss law, $\chi \sim 1/(T - T_F)$. This growth of χ is seen as a softening of specific elastic constants, which are determined by the symmetry of the model. For example, in the four-state model the shear elastic constant C_{1212} is softened as the transition to the rhombohedral state is approached. In the three-state model as well as in the dipolar six-state model C_{1111} is softened, whereas C_{1212} remains unaffected. Ordering of the orientations in the low-temperature phase has two effects: (a) a restiffening of the elastic constants which were softened upon approaching the transition and (b) the appearance of new elastic constants, reflecting the lower crystal symmetry of the low-temperature phase. In our models the transition to the homogeneously ordered state is always discontinuous. Hence the softening of the medium is disrupted at the transition temperature. In fact experiments on $\mathrm{K}_x\mathrm{TaO}_3(\mathrm{Li})_{1-x}$ show a softening of C_{1111} according to a Curie-Weiss law and no modification of C_{1212}.[38] Experiments on $(\mathrm{KBr})_x(\mathrm{KCN})_{1-x}$ for $x \sim 0.3$ reveal a pronounced minimum of C_{1212} at T_F, whereas C_{1111} is less temperature dependent.[44,42,21]

For the pure glass, the susceptibility shows Curie behavior $\chi \sim 1/T$, on approaching the glass transition. This gives rise to a softening of the same elastic constants as for the transition to the homogeneously ordered phase. Freezing in random directions disrupts the softening, but does not generate new elastic constants. The increase of the elastic constants sets in at T_G and reflects the decrease of the susceptibility due to a finite fraction of frozen spins q. At the same temperature, T_G, one observes a strong increase of the elastic peak (5.6), which is determined by the glass order parameter q.

If uniform interactions are present—as, for example, in $(\mathrm{KBr})_x(\mathrm{KCN})_{1-x}$ close to $x \sim x_c$—we expect Curie-Weiss behavior on approaching the glass-transition temperature from above. Hence the enhancement of the susceptibility and the corresponding softening of the elastic medium at the glass transition is strongest close to the multicritical point x_c and less and less pronounced as x decreases.

Other mechanisms have been proposed to explain the random freezing of orientations. Michel[16] and Bostoen and Michel[43] consider a higher-order coupling between translational and rotational degrees of freedom of the form $\epsilon\epsilon f(d)$ together with random static strains. Random strains alone give rise to a gradual freezing process and cannot account for a sharp glass transition. Higher-order couplings between ϵ and d can be generated in our model by the process of coarse graining. Here we have restricted ourselves to the lowest order couplings, because we identify the interaction between the orientations as the basic mechanism for the phase transitions. If higher-order couplings of the form $\epsilon f(d) f(d)$ are present, then a homogeneous freezing of the orientations can give rise to an even wider variety of crystalline phases than the model discussed here.

To summarize: The four-state model as well as the dipolar six-state model seem to be adequate descriptions of prototype orientational glasses. At present we do not know of any experimental realization of our quadrupolar six-state model. On the other hand it is plausible that lattice anisotropies may prefer face-diagonal orientations of defects. Our theoretical results indicate that such a system can show types of behavior which differ qualitatively from the hitherto studied systems, for example, the existence of several glass phases with different local symmetries.

Several extensions of our work are possible. Besides random fields, which have been proposed as a disordering mechanism, there are in general also random anisotropies, which can give rise to new ferroelastically ordered phases.[20] The wave-number dependence of the quasieleastic peak can be calculated. Thereby it is possible to check the experimental accessibility of local static order in the glassy phases. Finally it seems interesting to extend our approach to dynamics, in particular for dipolar systems, where many experimental data are available.

ACKNOWLEDGMENTS

We have benefited from interesting discussions with K.Knorr. This work has been supported by the Sonderforschungsbereich 345.

APPENDIX A: SYMMETRY OF GENERAL p-STATE GLASSES WITH GAUSSIAN DISORDER

Consider the uniform Potts system with Hamiltonian

$$H = -\sum_{(x,x')} J_{xx'} \sum_{\mu=1}^{p} n^{\mu}(x) n^{\mu}(x),$$

$$n^{\mu}(x) = \delta_{\mu r(x)}, \qquad \text{(A1)}$$

where $r(x)$ is the state of the Potts variable at site x. This system is usually randomized[19,24] by allowing fluctuations of the coupling strength $J_{xx'}$. Each pair of interacting variables remains Potts symmetric. Here we discuss the situation, which arises if Potts symmetry is not microscopic but only macroscopic. The Hamiltonian is then

$$H = -\sum_{(x,x')} \sum_{\mu\nu} n^{\mu}(x) J^{\mu\nu}_{xx'} n^{\nu}(x). \qquad \text{(A2)}$$

Macroscopic Potts symmetry means that ensemble-averaged correlations of J are symmetric, i.e.,

$$J_0^{\mu\nu} \equiv [J^{\mu\nu}_{xx'}] \overset{!}{=} J_0^{\pi(\mu)\pi(\nu)} \qquad \text{(A3)}$$

and

$$\begin{aligned} G^{\mu\nu\rho\sigma} &\equiv [J^{\mu\nu}_{xx'} J^{\rho\sigma}_{xx'}] - [J^{\mu\nu}_{xx'}][J^{\rho\sigma}_{xx'}] \\ &\equiv G^{\pi(\mu)\pi(\nu)\pi(\rho)\pi(\sigma)}, \end{aligned} \qquad \text{(A4)}$$

where $\pi(\mu)$ denotes a permutation of the states. $J_{xx'}$ is assumed to be statistically independent of $J_{yy'}$ unless $(xx') = (yy')$. The disorder is Gaussian, i.e., higher-order cumulants of J are zero.

The system (A2) is apparantly obtained by randomizing bonds, but it also contains hidden random field terms as we shall show now. Equation (A2) can also be written with another representation of Potts variables:

$$n^{\mu}(x) = \frac{1}{p}\{s^{\mu}(x) + 1\}. \qquad \text{(A5)}$$

Then

$$\begin{aligned} p^2 H &= -\sum_{(x,x')} \sum_{\mu\nu} \{s^{\mu}(x) + 1\} J^{\mu\nu}_{xx'} \{s^{\nu}(x) + 1\} \\ &= -\sum_{(x,x')} \sum_{\mu\nu} s^{\mu}(x) J^{\mu\nu}_{xx'} s^{\nu}(x) \\ &\quad -\sum_{x} \sum_{\mu} s^{\mu}(x) \left(\sum_{x'(\neq x)} \sum_{\nu} J^{\mu\nu}_{xx'} \right) \\ &\quad +\text{const.} \end{aligned} \qquad \text{(A6)}$$

Here we defined $J^{\nu\mu}_{x'x} \equiv J^{\mu\nu}_{xx'}$. The first term on the right-hand side of (A6) is a "real" random bond term. The second term contains $\sum_{x'(\neq x)} \sum_{\nu} J^{\mu\nu}_{xx'} = z \sum_{\nu} J_0^{\mu\nu} + \sum_{x'(\neq x)} \sum_{\nu} \delta J^{\mu\nu}_{xx'}$, where z is the coordination number. As $J_0^{\mu\nu}$ has Potts symmetry, $\sum_{\mu\nu} s^{\mu}(x) J_0^{\mu\nu} = 0$. The fluctuations $\delta J_{xx'}$ produce a random field $h^{\mu}(x) = \sum_{x'(\neq x)} \sum_{\nu} \delta J^{\mu\nu}_{xx'}$. It is well known that random fields alone cannot induce a glass transition. Furthermore the glass transition, which is induced by random exchange, is not destroyed by random fields, as long as the fluctuations in the exchange and the local field are uncorrelated. As far as the glass transition is concerned, we regard random fields as nongeneric terms. The transition to a phase with ferromagnetic long-range order may be suppressed by random fields, if they are sufficiently strong. This fact is well known from Ising models. However for Potts variables other types of ordered phases may be induced by random fields, provided that their distribution is chosen appropriately.[20]

In the following we require

$$\sum_{\mu} G^{\mu\nu\rho\sigma} = \cdots = \sum_{\sigma} G^{\mu\nu\rho\sigma} \qquad \text{(A7)}$$

so that no random field terms are present in the averaged Hamiltonian. From the definition of G we have

$$G^{\mu\nu\rho\sigma} = G^{\rho\sigma\mu\nu} \quad \text{and} \quad G^{\mu\nu\rho\sigma} = G^{\nu\mu\sigma\rho}. \qquad \text{(A8)}$$

The total number of p^4 entries of $G^{\mu\nu\rho\sigma}$ is reduced by conditions (A8). For the Potts glass the following constants are free:

$$p=2: \quad G^{1111}, G^{1122}, G^{1112}, G^{1212}, G^{1221}, \tag{A9}$$

$$p=3: \quad (\text{like } p=2) + G^{1123}, G^{1213}, G^{1231}, \tag{A10}$$

$$p \geq 4: \quad (\text{like } p=3) + G^{1123}, G^{1213}, G^{1231}. \tag{A11}$$

Condition (A7) further reduces the number of independent parameters. These can be chosen as

$$p=2: \quad G^{1212}, \tag{A12}$$

$$p=3: \quad G^{1212}, G^{1122}, G^{1221}, \tag{A13}$$

$$p \geq 4: \quad G^{1212}, G^{1122}, G^{1221}, G^{1111}. \tag{A14}$$

One can show that the order parameters of the system remain unchanged, if $G^{\mu\nu\rho\sigma}$ is replaced by $G^{\rho\nu\mu\sigma}$. Hence we choose the following independent parameters:

$$p=2: \quad G^{1212}, \tag{A15}$$

$$p=3: \quad G^{1212}, G^{1111}, \tag{A16}$$

$$p \geq 4: \quad G^{1212}, G^{1111}, G^{1122}. \tag{A17}$$

In the Ising case the SK model[45] is recovered, containing one disorder parameter G^{1212} which corresponds to the variance of the coupling strength $\sqrt{[(J_{xx'})^2]}$ in Ref. 45. For $p=3$ and $p \geq 4$ a general random bond model is described by two and three parameters, respectively.

The glassy phase of the six-state model in Sec. VI has been characterized by two disorder parameters J^+ and J^- (+ two homogeneous couplings). If microscopic symmetry is replaced by macroscopic symmetry, 10(!) parameters are needed to specify the quenched disorder, e.g.,

$$G^{1111}, G^{1144}, G^{1114}, G^{1414}, G^{1122},$$

$$G^{1422}, G^{1425}, G^{1212}, G^{1242}, G^{1245}. \tag{A18}$$

However we do not expect that all parameters reveal qualitatively new physical phenomena.

APPENDIX B: GINZBURG-LANDAU EXPANSION FOR THE FERROMAGNETIC TRANSITION

In the second-order cumulant expansion

$$z^{(\mathrm{inh})}\{Q,M,\bar{\epsilon}\} = \int \prod_x d^3u(x) \exp\left\{ -\tfrac{1}{2} \sum_x \sum_{\alpha\beta} \sum_{ijkl} \tilde{\epsilon}^{\alpha}_{ij}(x) \tilde{\epsilon}^{\beta}_{kl}(x) (\delta^{\alpha\beta} C^0_{ijkl} - \sum_{rs} F^{\alpha\beta}_{rs} K_{rij} K_{skl}) \right\} \tag{B1}$$

with

$$F^{\alpha\beta}_{ij} = \langle s^\alpha_i s^\beta_j \rangle_0 - \langle s^\alpha_i \rangle_0 \langle s^\beta_j \rangle_0 . \tag{B2}$$

Here the expectation values $\langle \cdots \rangle_0$ have to be calculated with z_0 *without* coupling to the homogeneous strain. As a first step we calculate $F^{\alpha\beta}_{ij}$. Three different quantities have to be calculated: $C_{ij} \equiv \langle s^\alpha_i s^\alpha_j \rangle_0$, $M^0_i \equiv \langle s^\alpha_i \rangle_0$, and $Q^0_{ij} \equiv \langle s^\alpha_i s^\beta_i \rangle_0$ for $\alpha \neq \beta$. As usual we introduce a Gaussian noise to decouple different replicas in z_0:

$$\ln z_0 = n \int_{-\infty}^{\infty} \left(\prod_i \frac{dy_i}{\sqrt{2\pi}} \right) \frac{1}{\sqrt{\det Q_{ij}}} \exp\left\{ -\tfrac{1}{2} \sum_{ij} y_i (Q^{-1})_{ij} y_j \right\} \ln z_1 + O(n^2) \equiv n \langle \ln z_1 \rangle_y + O(n^2) \tag{B3}$$

with

$$z_1 = \operatorname*{Tr}_{\{\vec{s}\}} \exp\left\{ J\vec{y}\cdot\vec{s} - \frac{J^2}{2} \sum_{ij} s_i s_j Q_{ij} + \hat{J}_0 \vec{s}\cdot\vec{M} \right\} . \tag{B4}$$

The expectation values are then given by

$$\begin{aligned} C_{ij} &= \langle \langle s_i s_j \rangle_1 \rangle_y , \\ M^0_i &= \langle \langle s_i \rangle_1 \rangle_y , \\ Q_{ij} &= \langle \langle s_i \rangle_1 \langle s_j \rangle_1 \rangle_y . \end{aligned} \tag{B5}$$

For the two-spin correlation we make the ansatz

$$C_{ij} = a I_{i1} I_{j1} + b I_{ij} \quad \text{for } p=3, \tag{B6}$$

$$C_{ij} = a I_{i1} I_{j1} + b \delta_{ij} \quad \text{for } p=4. \tag{B7}$$

Multiplying Eq. (B6) by $I_{i1} I_{j1}$ and summing over ij we find

$$a \sum_i I^2_{i1} \sum_j I^2_{j1} + b \sum_{ij} I_{i1} I_{j1} I_{ij} = \langle \langle \sum_i s_i I_{i1} \sum_j s_j I_{j1} \rangle_1 \rangle_y , \tag{B8}$$

$$\begin{aligned} a \times 3^2 \times 2^2 + b \times 3^2 \times 2 &= 3(\sqrt{3}\langle s_1 \rangle_0 + 2) \\ &= 6(M_0 + 1). \end{aligned}$$

Multiplying Eq. (B6) by I_{ij} and summing over ij we find

$$3^2 \times 2a + 3^2 \times 2b = 3 \times 2 \quad \text{or} \quad 3(a+b) = 1. \tag{B9}$$

Hence C_{ij} is determined by $\langle s_i \rangle_0 = M_0 e^1_i$

$$C_{ij} = \frac{1}{3} I_{ij} + \frac{M_0}{3} (I_{i1} I_{j1} - I_{ij}). \tag{B10}$$

If this result is substituted in Eq. (B1), the first term gives rise to a renormalization of the bare elastic constants at high temperatures and the second term vanishes due to cubic symmetry

$$\sum_{ij}\sum_{x}\langle\tilde{\epsilon}_{ii}(x)\tilde{\epsilon}_{jj}(x)\rangle(I_{i1}I_{j1}-I_{ij})=0. \tag{B11}$$

The argument for the four-state model is completely analogous.

To study the transition from the paramagnet to the collinear ferromagnet we calculate $\langle s_k\rangle_0$ perturbatively for small M and Q_L:

$$\begin{aligned}\langle s_k\rangle_0 = {} & \sum_{i}\hat{J}_0 M_i \frac{1}{p}\sum_{\mu} e_i^{\mu} e_k^{\mu}\\ & +\frac{1}{2}\sum_{ij}\hat{J}_0^2 M_i M_j \frac{1}{p}\sum_{\mu} e_i^{\mu} e_j^{\mu} e_k^{\mu}\\ & +O(M^3, M^2Q, Q^2),\end{aligned} \tag{B12}$$

with

$$\sum_{i} e_i^1 \frac{1}{p}\sum_{\mu} e_i^{\mu} e_k^{\mu} = e_k^1 \tag{B13}$$

and

$$\sum_{ij} e_i^1 e_j^1 \frac{1}{p}\sum_{\mu} e_i^{\mu} e_j^{\mu} e_k^{\mu} = (p-2)e_k^1. \tag{B14}$$

Hence we find

$$\langle s_k\rangle_0 = e_k^1 \hat{J}_0 M\left(1+(p-2)\hat{J}_0\frac{M}{2}\right) \tag{B15}$$

and therefore

$$\begin{aligned}&\langle s_i\rangle_0\frac{\partial}{\partial M}\langle s_j\rangle_0\\ &\quad = e_i^1 e_j^1 \hat{J}_0 M\left(1+(p-2)\hat{J}_0\frac{M}{2}\right)\hat{J}_0(1+(p-2)\hat{J}_0 M)\\ &\quad \approx e_i^1 e_j^1 \hat{J}_0^2 M(1+\tfrac{3}{2}(p-2)\hat{J}_0 M).\end{aligned} \tag{B16}$$

The contribution from $(\partial/\partial M)Q_{ij}^0$ is of higher order and can be neglected as long as we are only interested in linear and quadratic terms in M. Hence we find

$$\lim_{n\to 0}\frac{1}{n}\frac{\partial}{\partial M}\ln z_{\text{inh}} = \lim_{n\to 0}-\frac{1}{n}\sum_{rijskl}K_{rij}K_{skl}\sum_{x}(n\langle\tilde{\epsilon}_{ij}^{\alpha}(x)\tilde{\epsilon}_{kl}^{\alpha}(x)\rangle - n(n-1)\langle\tilde{\epsilon}_{ij}^{\alpha}(x)\tilde{\epsilon}_{kl}^{\beta}(x)\rangle)e_r^1 e_s^1 \hat{J}_0^2 M(1+\tfrac{3}{2}(p-2)\hat{J}_0 M) \tag{B17}$$

or explicitly for $p=3$

$$\frac{1}{2}\lim_{n\to 0}\frac{1}{n}\frac{\partial}{\partial M}\ln z_{\text{inh}} = -\frac{1}{2}\frac{\sigma^2}{3}\sum_{x}\sum_{ik}[\langle\tilde{\epsilon}_{ii}(x)\tilde{\epsilon}_{kk}(x)\rangle]e_i^1 e_k^1 \hat{J}_0^2 M(1+\tfrac{3}{2}\hat{J}_0 M)+O(M^3, MQ, Q^2) \tag{B18}$$

and for $p=4$

$$\frac{1}{3}\lim_{n\to 0}\frac{1}{n}\frac{\partial}{\partial M}\ln z_{\text{inh}} = -\sigma^2\hat{J}_0^2 M(1+3\hat{J}_0 M)\sum_{x}[\langle\tilde{\epsilon}_{23}(x)\tilde{\epsilon}_{23}(x)\rangle+\langle\tilde{\epsilon}_{31}(x)\tilde{\epsilon}_{31}(x)\rangle+\langle\tilde{\epsilon}_{12}(x)\tilde{\epsilon}_{12}(x)\rangle]+O(M^3, MQ, Q^2). \tag{B19}$$

The disconnected correlations $[\langle\tilde{\epsilon}_{ij}(x)\rangle\langle\tilde{\epsilon}_{kl}(x)\rangle]$ have been neglected because they are of higher order.

---

[1] U.T. Höchli, K. Knorr, and A. Loidl, Adv. Phys. **39**, 405 (1990).

[2] K. Binder and A.P. Young, Rev. Mod. Phys. **58**, 801 (1986).

[3] K.H. Michel and J. Naudts, Phys. Rev. Lett. **39**, 212 (1977); J. Chem. Phys. **67**, 547 (1977); **68**, 216 (1978).

[4] H. Vollmayr, R. Kree, and A. Zippelius, Europhys. Lett. **12**, 235 (1990).

[5] E.R. Grannan, M. Randeria, and J.P. Sethna, Phys. Rev. Lett. **60**, 1402 (1988); Phys. Rev. B **41**, 7784 (1990).

[6] I. Kanter and H. Sompolinski, Phys. Rev. B **33**, 2073 (1986).

[7] J.P. Sethna, S.R. Nagel, and Th. Ramakrishnan, Phys. Rev. Lett. **53**, 2489 (1984).

[8] K.H. Michel and J.M. Rowe, Phys. Rev. B **22**, 1417 (1980).

[9] K.H. Michel, Phys. Rev. Lett. **57**, 2188 (1986); Phys. Rev. B **35**, 1405 (1987); **35**, 1414 (1987).

[10] M. Born and K. Huang, *Dynamical Theory of Crystal Lattices* (Clarendon, Oxford, England, 1954).

[11] K.H. Michel, Z. Phys. B **54**, 129 (1984).

[12] L.D. Landau and E.M. Lifshitz, *Statistical Physics* (Pergamon, London, 1984).

[13] H. Kanzaki, Phys. Chem. Solids **2**, 24 (1957).

[14] R. deWit, Solid State Phys. **10**, 247 (1960).

[15] D. Hammes, H.O. Carmesin, and K. Binder, Z. Phys. B **76**, 115 (1989).

[16] K.H. Michel, Z. Phys. B **68**, 259 (1987).

[17] D. Sahu and S.D. Mahanti, Phys. Rev. Lett. **48**, 936 (1982); Phys. Rev. B **26**, 2981 (1982).

[18] K.H. Michel and T. Theuns, Phys. Rev. B **40**, 5761 (1989).

[19] D. Elderfield and D.J. Sherrington, J. Phys. C **16**, L497 (1983); **16**, L971 (1983); **16**, L1169 (1983).

[20] H. Vollmayr, R. Kree, and A. Zippelius, unpublished.

[21] A. Loidl, R. Feile, and K. Knorr, Z. Phys. B **42**, 143 (1981).

[22] F. Lüty, *Defects in Insulating Crystals*, edited by V.M. Tuckkevich and K.K. Shvarts (Springer, Berlin, 1981), p. 69.

[23] G.S. Parry, Acta Crystallogr. **15**, 596 (1962); **15**, 601 (1962).

[24] D.J. Gross, J. Kanter, and H. Sompolinsky, Phys. Rev. Lett. **55**, 304 (1985).

[25] H.J. Herrmann, Z. Phys. B **35**, 171 (1979).

[26] H.O. Carmesin, J. Phys. A **22**, 297 (1989).

[27] J. Banavar and M. Cieplak, Phys. Rev. B **39**, 9633 (1988).

[28] H.O. Carmesin and K. Binder, J. Phys. A **21**, 4053 (1988); M. Scheucher, J.D. Reger, K. Binder, and A.P. Young, Phys. Rev. B **42**, 6881 (1990).

[29] K.H. Michel and J.M. Rowe, Phys. Rev. B **32**, 5818 (1985).

[30] Y. Yacobi and S. Just, Solid State Commun. **15**, 715 (1974).

[31] U.T. Höchli and D.Baeriswyl, J. Phys. C **17**, 311 (1984).

[32] A. Cimino and G.S. Parry, Nuovo Cimento **19**, 971 (1960).

[33] M. Atoje, J. Chem. Phys. **54**, 3514 (1971).

[34] D.L. Price, J.M. Rowe, I.J. Rush, E. Prince, D.G. Hinks, and S. Susman, J. Chem. Phys. **56**, 3697 (1972).

[35] M. Sugisaki,T. Matsuo, H. Suga, and S. Seki, Bull. Chem. Soc. Jpn. **41**, 1747 (1968).

[36] G. Knopp, K. Knorr, A. Loidl, and S. Haussühl, Z. Phys. B **51**, 259 (1983).

[37] S.R. Andrews, J. Phys. C **18**, 1357 (1985).

[38] U.T. Höchli, H.E. Weibel, and W. Rehwald, J. Phys. C **15**, 6129 (1982).

[39] U.T. Höchli, P. Kofel, and M. Maglione, Phys. Rev. B **32**, 4546 (1985).

[40] M. Maglione, Ph.D. Thesis, EPF Lausanne 1987.

[41] M. Maglione, U.T. Höchli, and J. Joffrin, Phys. Rev. Lett. **57**, 436 (1986).

[42] J.M. Rowe, J.J. Rush, D.G. Hinks, and G. Susman, Phys. Rev. Lett. **43**, 1158 (1979).

[43] C. Bostoen and K.H. Michel, Z. Phys. B **71**, 369 (1988).

[44] K. Knorr and A. Loidl, Phys. Rev. Lett. **57**, 460 (1986).

[45] D. Sherrington and S. Kirkpatrick, Phys. Rev. Lett. **35**, 1792 (1975).